



2018

**A Novel, Orally Active Hydrogen Sulfide-Releasing Compound, SG1002, Improves Left Ventricular Function with an Associated Induction of Angiogenesis in a Murine Model of Ischemia/Reperfusion**

Om A. Evani  
*Virginia Commonwealth University*

Follow this and additional works at: <https://scholarscompass.vcu.edu/etd>

© Om Evani

---

**Downloaded from**

<https://scholarscompass.vcu.edu/etd/5389>

This Thesis is brought to you for free and open access by the Graduate School at VCU Scholars Compass. It has been accepted for inclusion in Theses and Dissertations by an authorized administrator of VCU Scholars Compass. For more information, please contact [libcompass@vcu.edu](mailto:libcompass@vcu.edu).

A NOVEL, ORALLY ACTIVE HYDROGEN SULFIDE-RELEASING COMPOUND, SG1002, IMPROVES  
LEFT VENTRICULAR FUNCTION WITH AN ASSOCIATED INDUCTION OF ANGIOGENESIS IN A  
MURINE MODEL OF MYOCARDIAL ISCHEMIA/REPERFUSION

A Thesis submitted in partial fulfillment of the requirements for the degree of Master of Science at  
Virginia Commonwealth University

by

OM EVANI  
B.A., Biology and Economics, University of Virginia, 2016

Director: FADI N. SALLOUM  
Associate Professor  
Department of Internal Medicine, Division of Cardiology  
VCU School of Medicine

Virginia Commonwealth University  
Richmond, VA  
May 2018

## Acknowledgements

I would like to express my appreciation and gratitude to a short list of people without whom this manuscript would not have been possible.

First, Dr. Fadi Salloum, my mentor and thesis advisor. I cannot express how grateful I am to have had your support, guidance, and patience over the course of the past year. You are somebody that I have truly come to respect and admire for your work-ethic and values. You will continue to be role model for me as I move forward in my journey.

I would like to thank my committee members, Dr. Abbate and Dr. Pittman, for taking the time out of their busy schedules to support me in my path to a successful year of research.

I would also like to thank the many professors in the physiology department at the VCU School of Medicine who helped me develop a strong foundation in the basic sciences over the past two years.

Dr. Charles Anderson, for being the most accessible (and brilliantly sarcastic) professor I have ever had – thank you for going out of your way to help push the boundaries of my, Laura, Scott, and Zach’s knowledge both during PHIS 501 and afterwards.

Drs. Clive Baumgarten and Roland Pittman, for first piquing my interest in cardiovascular physiology and research.

Dr. Jose Huizar, for giving me the opportunity to have my first experience in the operating room and to assist him with his research. You are a great example of a talented and compassionate physician and are somebody that I will strive to emulate in the future.

Dr. Ramzi Ockaili, for the opportunity to gain experience as his teaching assistant for the undergraduate students.

Dr. Anindita Das, for allowing me to fill up my water bottle at the cooler next to her office almost every day for the past year. And for always airing her grievances about the -80 freezer temperature to Teja instead of me.

Dr. Arun Samidurai and Dr. Rui Wang, for answering any and every molecular biology question that I posed to them.

Dr. Adolfo (Gabriele) Mauro, for helping me with the histological slide preparation and guiding me through the wonderful world of histological staining.

Bharat Balan, for mentoring me throughout CERT, introducing me to the Salloum lab, and showing me the ropes as he completed his Master’s project last year.

Teja Devarakonda, for teaching me almost everything I know about wet lab and for helping me troubleshoot various issues that I ran into during my project. I can’t thank you enough for putting up with my incessant questioning, even when it came at the most inconvenient times. You are a gentleman and a scholar!

Chad Cain, for his help in teaching me some of the ins and outs of mouse echocardiography and for creating those magical excel templates that save us countless hours of data compilation and processing.

Donatas Kraskauskas, for taking care of our supply center ordering and always coming through with a funny video to lighten the mood. He is also one of the most selfless and helpful people I have met – a true team player.

And most importantly, Mom, Dad, and Medha, for providing me with unconditional love and support for the last 23 years. I owe all of my success to you.

## Table of Contents

	Page
Acknowledgements.....	ii
List of Figures.....	iv
Abstract.....	v
<b>Introduction.....</b>	<b>1</b>
1.1 Background.....	1
1.2 Pathophysiology of Myocardial Ischemia/Reperfusion Injury.....	2
1.3 Mechanisms of Adverse Remodeling.....	2
1.4 Mechanism of Angiogenesis.....	4
1.5 Hydrogen Sulfide in the Cell.....	7
1.6 Hydrogen Sulfide in Cardioprotection.....	8
1.7 Therapeutic Applications of H <sub>2</sub> S.....	12
1.8 Primary Objective of Experimentation.....	13
<b>Methods and Materials.....</b>	<b>14</b>
2.1 Chemicals and Reagents.....	14
2.2 Animals.....	14
2.3 Experimental Groups.....	14
2.4 Murine Ischemia/Reperfusion Model.....	16
2.5 Echocardiography.....	17
2.6 Measurement of Electrocardiographic Parameters.....	17
2.7 Western Blotting.....	17
2.8 Quantitative Real-Time PCR.....	18
2.9 Histology.....	18

2.10	Data Analysis.....	19
<b>Results.....</b>		<b>20</b>
3.1	Effect of H <sub>2</sub> S on LV Function.....	20
3.2	Effect of H <sub>2</sub> S on QRS Interval.....	20
3.3	Effect of H <sub>2</sub> S on capillary density at 7 days and 28 days.....	20
3.4	Effect of H <sub>2</sub> S on VEGF-A mRNA levels 28 days post IR.....	21
3.5	Effect of H <sub>2</sub> S on Angiopoietin-1 mRNA levels 28 days post IR.....	21
3.6	Effect of H <sub>2</sub> S on microRNA-126 levels at 28 days post IR.....	21
3.7	Effect of H <sub>2</sub> S on VEGF-A protein levels at 7 and 28 days post IR.....	21
<b>Discussion.....</b>		<b>33</b>
<b>References.....</b>		<b>38</b>

## List of Figures

	Page
Figure 1: Vicious Cycle of Heart Failure.....	3
Figure 2: Schematic Overview of the Mechanism of Angiogenesis.....	6
Figure 3: Mechanism of H <sub>2</sub> S in Induction of Angiogenesis.....	11
Figure 4: Experimental Design.....	15
Figure 5 H <sub>2</sub> S preserves ejection fraction at 28 days post IR .....	22
Figure 6: H <sub>2</sub> S treatment attenuates QRS complex widening at 28 days post IR.....	23
Figure 7: H <sub>2</sub> S therapy increases vascular density at 7 days post IR.....	24
Figure 8: H <sub>2</sub> S therapy increases vascular density at 28 days post IR.....	25
Figure 9: H <sub>2</sub> S slightly increases peri-infarct region capillary density at 28 days post IR.....	26
Figure 10: H <sub>2</sub> S slightly increases non-infarct region capillary density at 28 days post IR.....	27
Figure 11: SG1002 slightly increases VEGF-A mRNA levels at 28 days post IR.....	28
Figure 12: SG1002 slightly increases Angiopoietin-1 mRNA levels at 28 days post IR.....	29
Figure 13: SG1002 significantly increases microRNA-126 levels at 28 days post IR.....	30
Figure 14: H <sub>2</sub> S therapy increases VEGF-A protein expression at 7 days post IR.....	31
Figure 15: H <sub>2</sub> S therapy increases VEGF-A protein expression at 28 days post IR.....	32

## **Abstract**

A NOVEL, ORALLY ACTIVE HYDROGEN SULFIDE-RELEASING COMPOUND, SG1002, IMPROVES LEFT VENTRICULAR FUNCTION WITH AN ASSOCIATED INDUCTION OF ANGIOGENESIS IN A MURINE MODEL OF MYOCARDIAL ISCHEMIA/REPERFUSION

By Om Evani

A Thesis submitted in partial fulfillment of the requirements for the degree of Master of Science at  
Virginia Commonwealth University

Virginia Commonwealth University, 2018

Director: Fadi N. Salloum, Ph.D., F.A.H.A.  
Associate Professor  
Department of Internal Medicine, Division of Cardiology  
VCU School of Medicine

Hydrogen sulfide ( $\text{H}_2\text{S}$ ) is the newest member of the gasotransmitter family and is becoming well known for its cardioprotective effects in preclinical trials. Many recent studies have shown the benefits of exogenous  $\text{H}_2\text{S}$  in the setting of acute myocardial infarction (AMI) and pressure overload-induced heart failure, but current formulations are derived from inorganic salts which have shortcomings in the precision and control of release of  $\text{H}_2\text{S}$ . The main objective of this thesis was to determine if the novel, orally active, slow-releasing compound, SG1002, can attenuate the severity of damage and adverse remodeling caused by ischemia/reperfusion injury through an induction of angiogenesis. A traditional sodium salt,  $\text{Na}_2\text{S}$ , which has been previously shown to be cardioprotective, was used as a positive control. SG1002 improved overall left ventricular function as measured by increased ejection fraction from echocardiography and decreased QRS interval from electrocardiography compared to untreated animals following MI. SG1002 therapy was also associated with an induction of angiogenesis, which was



determined through qRT-PCR, western blot, and histological methods. SG1002 increased VEGF protein levels, which was paralleled with an increase in capillary density in the infarct region. SG1002 also upregulated microRNA-126, which is thought to repress the inhibitor of VEGF, Spred-1. It is possible that this “angiomiR” plays a key role in the angiogenesis-related cardioprotection of H<sub>2</sub>S. The combination of increased pro-angiogenic factors along with greater vascular density resulting from SG1002 therapy indicates the therapeutic potential for this drug in the prevention and/or treatment of ischemic heart failure.

## Introduction

### **1.1 Background**

Heart failure is a complex clinical syndrome that serves as the final common pathway of many cardiac conditions. It is defined by the clinical presentation resulting from an inability of the heart to pump blood at a rate that is sufficient to meet the metabolic demands of the body. It is currently a global epidemic with >37.7 million individuals affected worldwide.<sup>1</sup> In America, about 6.5 million people above the age of 20 have heart failure, and approximately 960,000 new cases are diagnosed each year.<sup>2</sup> The number of annual hospitalizations for acute heart failure is rising due to the aging of the general population and the increasing prevalence of heart failure. The readmission rates also remain high, indicating the lack of progress made to attenuate the chronic course of this disease.<sup>3</sup> Despite significant advances in pharmacotherapy, coronary revascularization, and cardiac resynchronization therapy, patient outcomes remain poor with a 5-year survival rate of approximately 50% and a 10-year survival rate of approximately 10%.<sup>2,3</sup>

A variety of risk factors including obesity, diabetes, hypercholesterolemia, and hypertension can contribute to the development of heart failure. The most common cause of heart failure, accounting for one-third to two-thirds of all cases, is impaired left ventricular function secondary to coronary artery disease (CAD), a phenomenon known as ischemic cardiomyopathy.<sup>3</sup> In CAD, the arteries that supply blood to the heart muscle become hardened and narrowed due to plaque buildup over time. This atherosclerosis allows less blood to perfuse the heart, leading to decreased oxygen availability in the heart and damage to the cardiomyocyte.

### **1.2 Pathophysiology of Myocardial Ischemia-Reperfusion Injury**

During ischemia, the cardiomyocyte is unable to proceed through oxidative phosphorylation, resulting in decreased energy reserves, increased anaerobic glycolysis, and lactic acid buildup.<sup>4</sup> The accumulation of lactic acid causes a severe reduction in the cell's pH and in turn disrupts many ion

channels within the cell. One of the main channels affected is the  $\text{Na}^+/\text{K}^+$ -ATPase, which is responsible for maintaining the driving force of sodium into the cell. The disruption of the  $\text{Na}^+/\text{K}^+$ -ATPase leads to a buildup of sodium within the cell and eventual reversal of the  $\text{Na}^+/\text{Ca}^{2+}$  antiporter, another important ion channel within the cardiomyocyte. Under normal conditions, the  $\text{Na}^+/\text{Ca}^{2+}$  antiporter extrudes one calcium from the cell for every three sodium ions that enter it. However, reversal of the channel leads to an accumulation of cytosolic and mitochondrial calcium levels, causing dysfunction.<sup>4</sup>

Initially, the damage to the cell is reversible and the restoration of blood flow during this period will lead to recovery of the normal structures and function. If ischemia persists for an extended period of time, the damage becomes irreversible and cell death occurs. Prior to cell death, there is a period of time when the ischemic myocyte is viable but vulnerable to further injury if blood flow is restored, also known as reperfusion injury.<sup>5</sup> Because of the decreased pH level within the cell, the respiratory complexes of the mitochondrial transport chain are in the reduced state and produce a surge of reactive oxygen species (ROS) upon reperfusion.<sup>6</sup> These superoxide radicals can cause enzyme inactivation and lipid peroxidation. The reperfusion injury can cause reversible contractile abnormalities, known as “myocardial stunning.” However, reperfusion-induced death of cardiomyocytes that were viable at the end of the ischemic event is defined as lethal myocardial reperfusion injury.<sup>4</sup>

### **1.3 Mechanisms of Adverse Remodeling**

Cardiac remodeling refers to the alterations in the size, shape, and function of the heart resulting in molecular, cellular, and interstitial changes. Ventricular remodeling often occurs in response to cardiac injury (e.g. myocardial infarction), pressure overload (e.g. hypertension), or volume overload (ex. valvular regurgitation).<sup>7</sup> Although slight remodeling can be adaptive, as in the case of exercise, the overall remodeling following an injury such as a myocardial infarction (MI) is maladaptive. After a MI, there is an initial adaptive remodeling of tissue repair and scar formation, elongation, and thinning of the infarcted zone shortly following the injury.<sup>8–10</sup> Left ventricular volume also

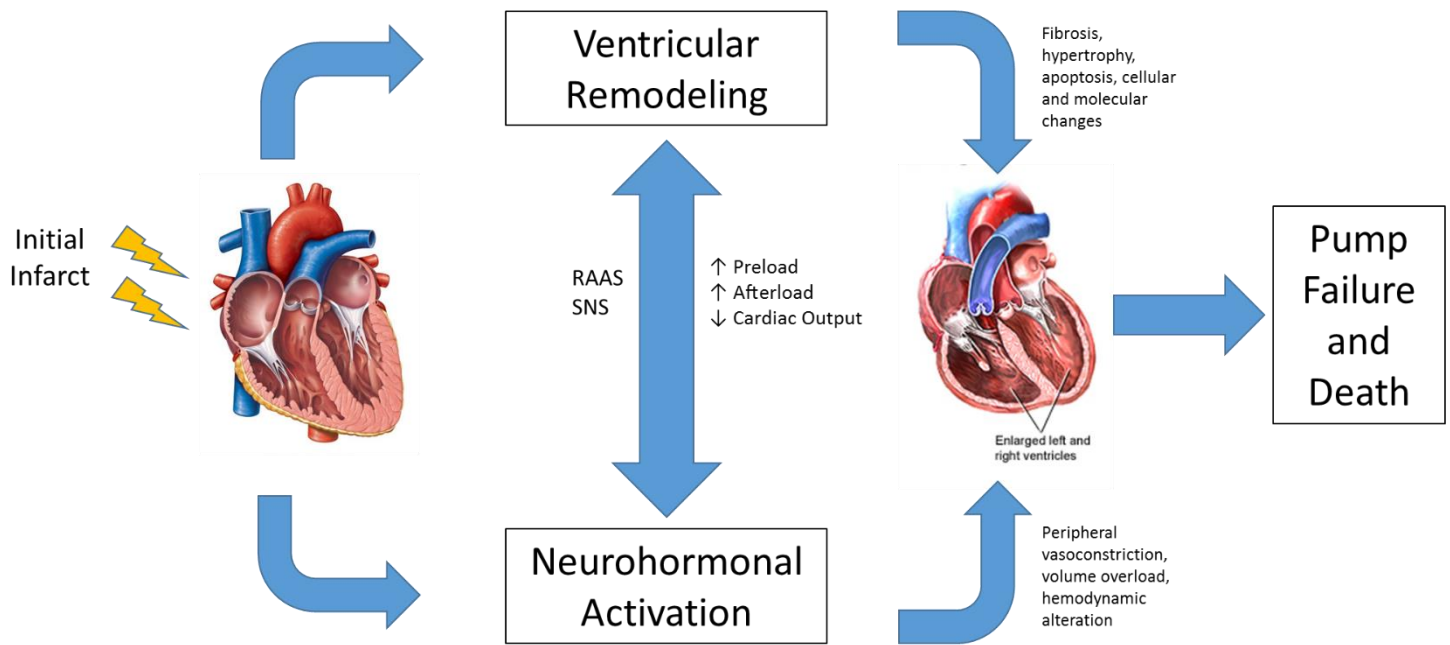


**Figure 1: Vicious cycle of heart failure.** The initial cardiac injury leads to concomitant processes of ventricular remodeling and neurohormonal activation caused by ventricular dysfunction. This leads to the clinical manifestations of heart failure and ultimately to pump failure and death.

increases in order to maintain the normal cardiac output and stroke volume.<sup>9</sup> Following the initial remodeling, the loss of contractile tissue in the infarct zone leads to elongation and hypertrophy of the surviving cardiomyocytes in the non-infarcted zone, which increases ventricular wall circumference and sphericity. The increase in wall stress and wall thickness can then lead to an imbalance of oxygen supply and demand, further exacerbating the problem.<sup>11</sup> The magnitude of the remodeling changes observed relates directly to the infarct size, with larger infarcts resulting in greater dilation and greater increases in systolic and diastolic stress.<sup>12</sup>

Neurohormonal activation in heart failure is known to regulate compensatory changes in response to decreased cardiac output, but it is also a major contributor to the progression of the disease. Some of the most important hormones involved are norepinephrine from the adrenergic nervous system, aldosterone from the renin-angiotensin-aldosterone axis (RAAS), and antidiuretic hormone (ADH).<sup>13</sup> These hormones are initially beneficial in fluid retention and vasoconstriction to maintain cardiac output and blood pressure, but their sustained activation ultimately prove harmful by increasing the load on the failing heart. Other detrimental factors include oxidative stress, pro-inflammatory cytokines, and endothelin.<sup>9</sup>

#### **1.4 Mechanism of Angiogenesis**

One way that the heart adapts following an injury is the induction of angiogenesis, the budding of capillaries that leads to the formation of new microvessels from pre-existing vascular structures.<sup>14</sup> In fact, one of the ultimate determinants of infarct size and the amount of viable myocardium after acute ischemic injury is the extent of collateral blood flow within the occluded vascular bed.<sup>15</sup> The formation of new blood vessels involves several steps. First, there is breakdown of the collagen underlying the endothelium by the matrix metalloproteinases (MMPs), a family of secreted and membrane-associated endopeptidases.<sup>16</sup> The loss of collagen leads to irreversible dissolution of the matrix, and this fragmentation of the basement membrane is carried out by MMP-2 and MMP9, which are secreted by

endothelial cells.<sup>17</sup> MMP-1, an interstitial collagenase, is also required for angiogenesis.<sup>18</sup> The dissolution of the underlying matrix allows endothelial cells to migrate, adhere and proliferate. The migration of endothelial cells is driven by a gradient of vascular endothelial growth factor (VEGF), and their adhesion involves the interaction between the  $\alpha_v\beta_3$  integrin and the extracellular matrix.<sup>19,20</sup> Finally, there is formation and maturation of a new three-dimensional tubular structure to support the flow of blood. A number of different factors – chemical, molecular, or mechanical – can stimulate angiogenesis and influence each step of the process.<sup>21</sup>

The molecular machinery that initiates angiogenesis may be driven by deprivation of oxygen and other important nutrients. Hypoxia-inducible transcription factors, such as hypoxia-inducible factor-1 $\alpha$  (HIF-1 $\alpha$ ), mediate the cardiomyocyte's adaptation to hypoxia and have been associated with the presence of collaterals in patients with CAD.<sup>22</sup> HIF-1 $\alpha$  is expressed in cardiomyocytes and endothelial cells early after MI, and its expression can persist up to 4 weeks after MI.<sup>23</sup> The HIF pathway upregulates a host of pro-angiogenic genes including VEGF, angiopoietin-1, angiopoietin-2, platelet-derived growth factor (PDGF) and basic fibroblast growth factor (bFGF).<sup>24</sup> These angiogenic factors bind to cognate receptors that are expressed on the surface of vascular endothelial cells and are involved in increasing vascular permeability, endothelial cell proliferation, sprouting, migration, adhesion, and tube formation.

In addition to ischemia, another important contributor to angiogenesis is inflammation. MI rapidly induces a large influx of inflammatory cells into ischemic area and studies show that their presence is sufficient to produce angiogenesis.<sup>25</sup> Following infarction, leukocyte infiltration can release numerous cytokines (TGF- $\beta$ , IL-1 $\beta$ , and IL-6) which are capable of stimulating VEGF expression and release. VEGF, in turn, can stimulate and recruit other macrophages to supplement the inflammatory response. The combination of leukocyte-derived influx of cytokines, as well as synthesis of bFGF, VEGF, and MMPs provide a suitable environment for new vessel development.<sup>25</sup> Endothelial cells also act as mechanoreceptors, sensing and responding to changes in wall stress. Myocardial stretch due to

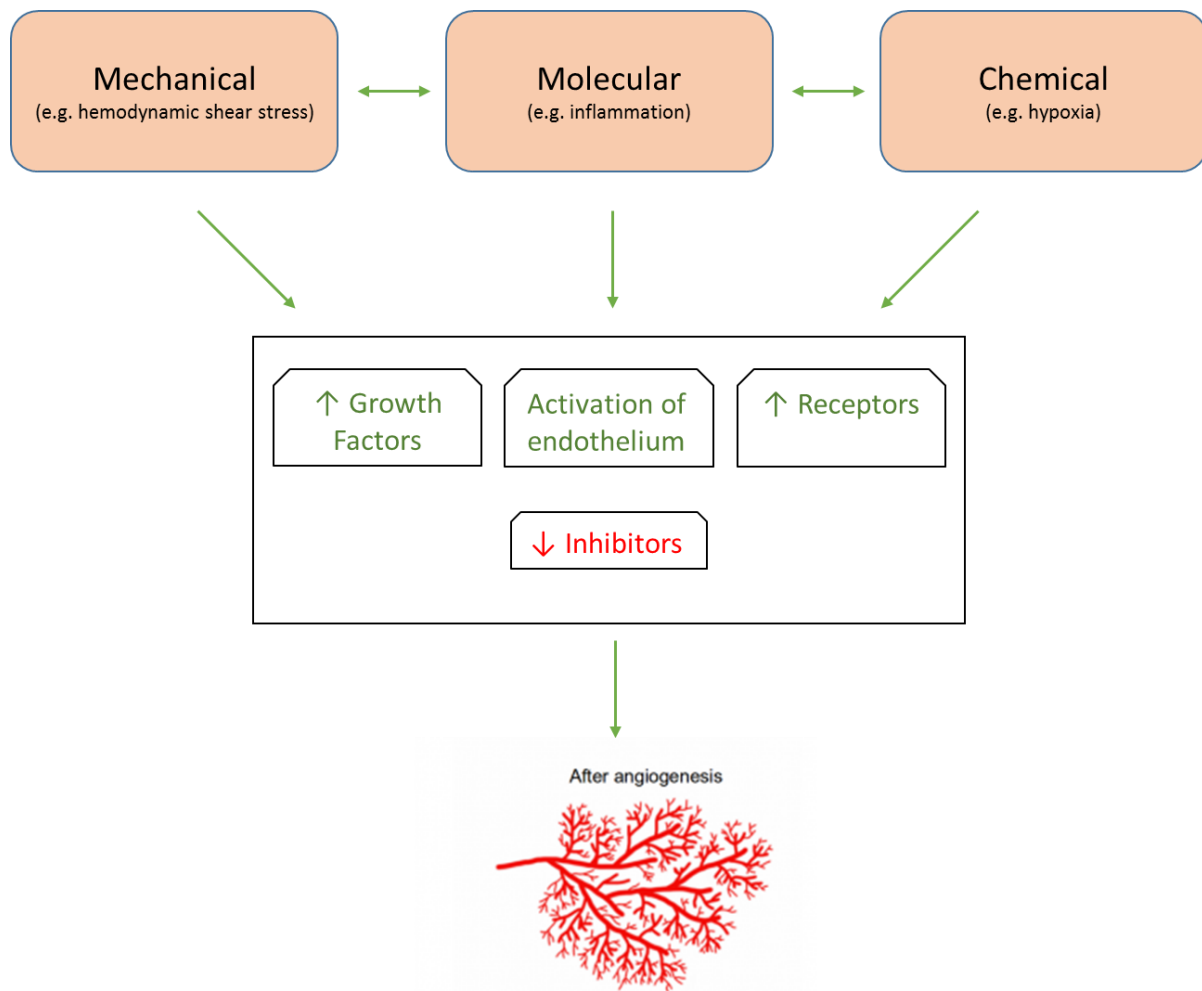


**Figure 2: Schematic overview of the mechanism of angiogenesis.** Mechanical, molecular, or chemical stressors can induce activation of the endothelium, production of growth factors, and repression of inhibitors. These steps lead to formation of new microvessels from pre-existing vascular structures.

augmentation of blood flow through the vessel is associated with a rapid induction of VEGF gene expression mediated by TGF- $\beta$  release.<sup>26</sup> Increased blood flow also decreases leukocyte adhesion to the endothelium through the downregulation of vascular cell adhesion molecule-1 (VCAM-1) expression.<sup>27,28</sup>

### **1.5 Hydrogen Sulfide in the Cell**

Hydrogen sulfide ( $H_2S$ ) was long thought to be little more than a toxic gas. However, similar to nitric oxide (NO) and carbon monoxide (CO), it has more recently been shown to be an endogenous gas within the body that exerts physiological functions.<sup>29</sup> As a gaseous signaling molecule,  $H_2S$  has the ability to diffuse freely across cell membranes in a receptor-independent manner and activate various signaling targets. The bulk of its production within the cell is mediated by three enzymes: cystathionine- $\beta$ -synthase (CBS), cystathionine- $\gamma$ -lyase (CSE) and 3-mercaptopyruvate sulfurtransferase (3-MST). CBS and CSE work in a tissue specific manner. CBS expression is the primary physiological source of  $H_2S$  in the central nervous system, while CSE is the main producer of  $H_2S$  in the cardiovascular system. CSE is a pyridoxal-5-phosphate-(PLP-) dependent enzyme located in the cytosol, and it uses L-cysteine as the principal substrate to produce  $H_2S$ . MST is also present within cardiomyocytes and works together with another enzyme, cysteine aminotransferase (CAT), to produce sulfane sulfur, or bound sulfur. This can subsequently form  $H_2S$  through reduction of the atomic sulfur or release from thiosulfate or persulfides.<sup>29</sup>

### **1.6 Hydrogen Sulfide and Cardioprotection**

$H_2S$  has been a great source of interest in respect to cardiovascular disease since its discovery as a physiologically relevant molecule. A landmark study in 2007 showed the infarct-sparing effects of hydrogen sulfide either from overexpression of myocardial CSE or exogenous administration of  $Na_2S$ , a  $H_2S$  donor.<sup>30</sup>  $H_2S$  also has a large potential for clinical translatability as a study showed that plasma levels of  $H_2S$  in patients with CAD were significantly lower than those observed in control patients with normal angiography.<sup>31</sup> Another recent clinical study showed that total plasma sulfide levels have been



negatively related to severity of congestive heart failure, with the lowest levels seen in NYHA Class IV heart failure patients.<sup>32</sup> Since the initial findings of H<sub>2</sub>S as a cardioprotective agent, a vast amount of research has gone into investigating the various mechanisms through which it acts.

#### Anti-apoptotic effects

In addition to infarct size, apoptotic cell death also plays an important role in the cardiac remodeling process following ischemia-reperfusion (I/R) injury. A porcine model of I/R showed that therapeutic administration of H<sub>2</sub>S prior to the onset of reperfusion diminished the ensuing pro-apoptotic signaling.<sup>33</sup> Apoptotic signals during reperfusion have been linked to c-Jun N-terminal kinase (JNK) and p38 mitogen activated protein kinase (p38 MAPK) expressions, while anti-apoptotic signals are mediated by extracellular signal-regulated protein kinase 1 and 2 (Erk 1/2), protein kinase B (Akt), phosphoinositide-3-kinase (PI3K), and glycogen synthase kinase-3 $\beta$  (GSK-3 $\beta$ ).<sup>34</sup> A study utilizing primary cultured rat neonatal cardiomyocytes subjected to hypoxia/reoxygenation showed that H<sub>2</sub>S treatment attenuated early JNK phosphorylation and induction of apoptosis, which was paralleled with an increase in the anti-apoptotic Bcl-2 expression.<sup>35</sup> Similarly, in a model of doxorubicin-induced cardiotoxicity, H<sub>2</sub>S protected H9c2 cells by inhibition of the p38 MAPK pathway.<sup>36</sup> On the other hand, exogenous NaHS offered cardioprotection after hypoxia/reoxygenation injury through the phosphorylation of Erk1/2, PI3K, Akt, and GSK-3 $\beta$ .<sup>37</sup> A study also showed that Na<sub>2</sub>S attenuated apoptosis secondary to ischemia in adult isolated cardiomyocytes via induction of anti-apoptotic microRNA-21 expression.<sup>38</sup> The key role of microRNA-21 was further supported when the benefits were lost in cardiomyocytes treated with antagomiR-21 or those lacking microRNA-21 via genetic deletion.

#### Anti-oxidant effects

Oxidative stress is a cellular process that occurs due to a discordancy between oxidant and antioxidant systems.<sup>39</sup> It perpetuates the damage of the initial cardiac injury and promotes cell death. The presence of ROS alters the normal cellular function via lipid peroxidation, oxidation of proteins, and

DNA damage. H<sub>2</sub>S has been reported to act as a direct scavenger of ROS through its role as an electron donor and to activate several antioxidant enzymes.<sup>39</sup> Following chronic myocardial ischemia or I/R injury, H<sub>2</sub>S attenuated oxidative stress and mitochondrial dysfunction through the increase of nuclear localization of nuclear-factor-E2-related factor (Nrf2).<sup>40</sup> This finding was also corroborated in protecting the diabetic heart against I/R injury in db/db mice.<sup>41</sup> Nrf2 was found to be a transcription factor that regulates the gene expression of a number of antioxidant enzymes, including heme oxygenase-1 (HO-1) and thioredoxin 1 (Trx 1), by binding to the antioxidant responsive element (ARE) in the promoter region of certain genes. This binding subsequently activated induction of the endogenous antioxidant proteins and increased mitochondrial biogenesis. Exogenous H<sub>2</sub>S has also been shown to reduce ROS levels in rat neonatal cardiomyocytes following hypoxia/reoxygenation through inhibition of mitochondrial complex IV activity and increased activity of superoxide dismutases.<sup>42</sup>

#### Anti-inflammatory effects

I/R injury triggers an intense inflammatory response that begins as an adaptive process necessary for cardiac repair but is then implicated in the pathogenesis of post-infarction remodeling and heart failure.<sup>43</sup> The initial inflammatory reaction clears dead cells and extracellular matrix debris. The released debris promotes recruitment and formation of the inflammasome, a macromolecular structure comprised of apoptosis speck-like protein containing a caspase-recruitment domain (ASC), cryopyrin (NLRP3), and caspase-1. The inflammasome then amplifies the inflammatory response through activation of caspase-1 and the subsequent release of pro-inflammatory cytokines, interleukin (IL)-1 $\beta$  and IL-18.<sup>44</sup> H<sub>2</sub>S has been shown to limit leukocyte transmigration and to suppress the release of pro-inflammatory mediator tumor necrosis factor-alpha (TNF- $\alpha$ ) and cytokine IL-1 $\beta$ .<sup>30,33</sup> In H9c2 cells, H<sub>2</sub>S also produced an anti-inflammatory effect following lipopolysaccharide (LPS) stimulation through the impairment of nuclear factor- $\kappa$ B (NF- $\kappa$ B) signaling and activation of the PIK3/Akt pathway.<sup>45</sup> In the post-

ischemic mouse heart, H<sub>2</sub>S has been found to attenuate both the formation of the inflammasome and activation of caspase-1 via induction of microRNA-21.<sup>38</sup>

#### Pro-Angiogenic effects

H<sub>2</sub>S seems to exert its pro-angiogenic effects in the setting of wound healing through two main mechanisms: PI3K/Akt pathway and K<sub>ATP</sub> channel/p38 MAPK pathway.<sup>46,47</sup> Akt is activated by various extracellular signals and has been reported to increase endothelial cell proliferation, migration and tube formation. NaHS treatment induced an increase in Akt phosphorylation in endothelial cells, while this effect was decreased with PI3K inhibitors.<sup>46</sup> In a model of hindlimb ischemia, NaHS enhanced vascular endothelial growth factor (VEGF) synthesis in addition to VEGF activation, which further promoted phosphorylation of Akt.<sup>48</sup> For the second mechanism, endothelial cells express K<sub>ATP</sub> channels both in the plasma membrane and intracellular organelles. ATP-sensitive potassium channels are regulated by a variety of physiologic factors such as hypoxia and ischemia as well as by hormone levels. H<sub>2</sub>S has been shown to increase migration of endothelial cells, while inhibition of K<sub>ATP</sub> channel diminished the migratory response of endothelial cells.<sup>47</sup>

Angiogenesis also plays an important role in preventing the transition from compensatory hypertrophy to heart failure. In a mouse model of aortic banding for up to eight weeks, exogenous NaHS administration was associated with an increase in the expression of MMP-2, cluster of differentiation 31 (CD31), and VEGF, while there was a decrease in the expression of MMP9, endostatin, angiostatin, and tissue inhibitor of metalloproteinase-3 (TIMP-3).<sup>49</sup> Overall, the NaHS treated group showed a reduction in cardiac fibrosis and an improvement in function compared to control animals. In a model of pressure overload, diallyl trisulfide (DATS) increased the expression of VEGF and eNOS phosphorylation while decreasing angiostatin.<sup>50</sup> In a study with transverse aortic constriction (TAC) for 12 weeks, treatment of wild-type mice with H<sub>2</sub>S up-regulated the VEGF-Akt-eNOS-NO-cGMP pathway and mitigated the progression from compensated to decompensated heart failure.<sup>51</sup>

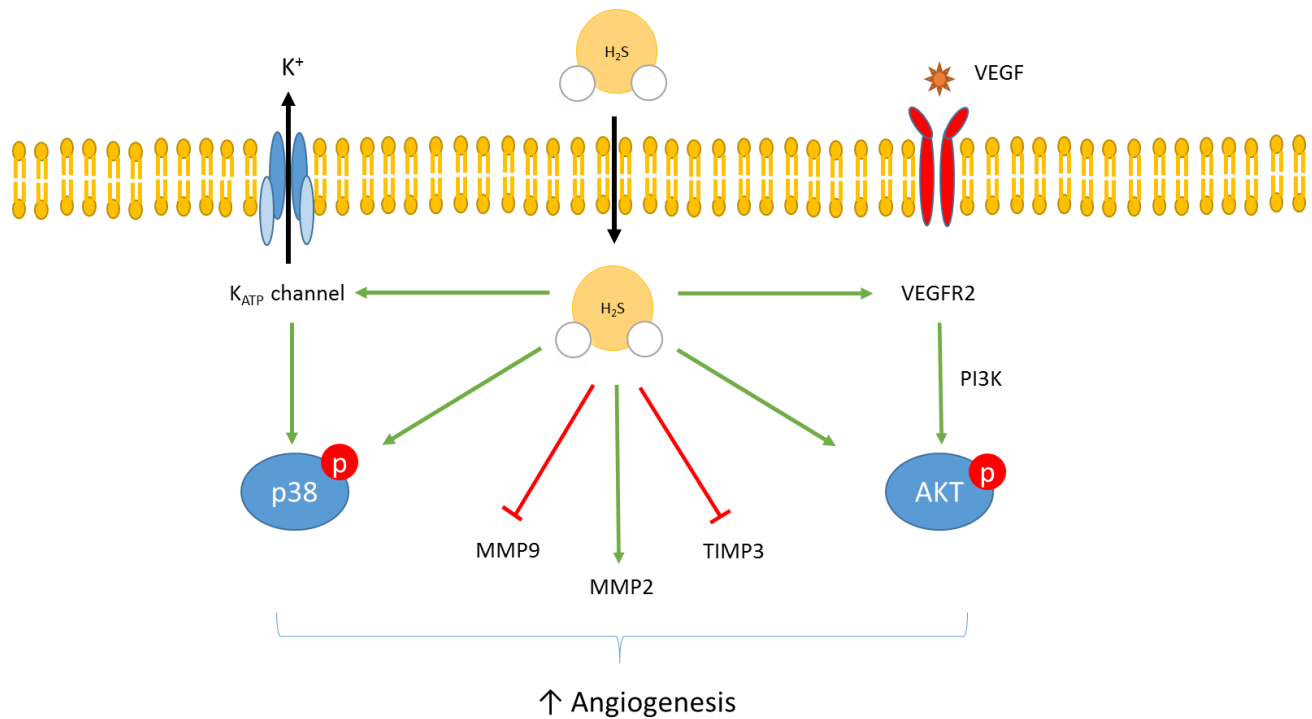


**Figure 3: Mechanisms of H<sub>2</sub>S in Induction of Angiogenesis.** H<sub>2</sub>S seems to exert its pro-angiogenic effects in the setting of wound healing through two main mechanisms: PI3K/Akt pathway and K<sub>ATP</sub> channel/MAPK pathway. H<sub>2</sub>S can also mitigate the anti-angiogenic MMP9/TIMP3 while activating MMP2.

## 1.7 Therapeutic Applications of H<sub>2</sub>S

### Fast-release donors

The most common fast-delivering compounds used as H<sub>2</sub>S donors rely on derivations from inorganic salts, such as Na<sub>2</sub>S and NaHS, in solution. In the past, these salts have been shown to confer cardioprotection as pre- and post-conditioning measures in regards to ischemia-reperfusion injury.<sup>38,52</sup> However, although these salts are soluble in water and their donation is rapid upon reaction, H<sub>2</sub>S is very unstable in solution because it can be easily oxidized.<sup>53</sup> In addition, a burst-like release of H<sub>2</sub>S in the plasma is contrary to how the molecule is endogenously synthesized within the body.<sup>54</sup> Increasing the concentration of H<sub>2</sub>S instantly can be associated with concentrations that are too high and can potentially be cytotoxic to the cell via inhibition of Complex IV in the mitochondria.<sup>53</sup> Moreover, the impurity of the commercially available H<sub>2</sub>S-releasing inorganic salts is a concern. Because a major challenge for utilizing H<sub>2</sub>S fast-releasing compounds is the difficulty in achieving the desired final concentration without it being released in waveform-like concentration fluctuations, many researchers have progressed towards the investigation of slow-releasing H<sub>2</sub>S donors.

### Slow-release donors

Diallyl trisulfide (DATS) is a stable donor of H<sub>2</sub>S that is commonly found in naturally occurring foods such as garlic. DATS has been shown to be a cardioprotective agent to treat myocardial I/R injury and pressure-overload heart failure.<sup>50,55</sup> However, one setback for future translatability is that DATS is derived from allicin, which is unstable in water.<sup>56</sup> One promising slow-release donor that has been investigated is GYY4137, which is a water-soluble compound that releases H<sub>2</sub>S upon hydrolysis. GYY4137 has been shown to exert vasodilatory and antihypertensive effects in preclinical studies.<sup>57</sup> A very interesting aspect of GYY4137 is that it is released preferentially in acidic conditions, which could allow for preferential H<sub>2</sub>S release in the ischemic tissue.<sup>58</sup>

Another promising slow-release H<sub>2</sub>S donor is SG1002. SG1002 is a novel, orally active, slow-releasing prodrug that has been gaining significant attention in cardiovascular medicine because of its ability to produce sustained and consistent levels of H<sub>2</sub>S in the plasma.<sup>59</sup> Pre-clinical studies have begun elucidating the cardioprotective effects of SG1002. Following TAC in mice, SG1002 was shown to reduce oxidative stress, preserve mitochondrial function and increase vascular density in the myocardium through induction of the VEGF-Akt-eNOS-cGMP pathway.<sup>51</sup>

SG1002 has also been shown to be well tolerated in a phase 1 clinical trial studying its safety and changes in serum H<sub>2</sub>S and NO levels.<sup>60</sup> At higher drug doses of 400 and 800 mg, SG1002 was well tolerated with minimal side effects. Both serum nitrates and serum H<sub>2</sub>S were increased in control and heart failure patients. Peak levels of serum H<sub>2</sub>S remained well below the toxic range at 1.1 μM. A phase 2 trial for assessment in 50 heart failure patients has been planned for the future to examine the ability of chronic SG1002 administration (3 months) to elevate H<sub>2</sub>S, reduce oxidative stress, and ultimately improve cardiac function.<sup>58,60</sup>

### **1.8 Primary Objective of Experimentation**

The objective of this thesis is to study the effect of H<sub>2</sub>S on adverse cardiac remodeling following myocardial ischemia/reperfusion injury in mice. One goal in particular is to study the orally bioavailable, slow-releasing H<sub>2</sub>S donor, SG1002, and its potential ability to confer cardioprotection through induction of angiogenesis.

## **Materials and Methods**

### **2.1 Chemicals and Reagents**

SG1002 was obtained from Sulfagenix (Cleveland, OH). 275 milligrams of SG-1002 was repelleted into each kilogram of Tekland Rodent Chow #7012 by Research Diets, Inc. SG was administered in the diet to reach dosages of 40 mg/kg/day.

For Western Blot, primary antibodies for VEGF and angiopoietin were purchased from Santa Cruz Biotechnology (Santa Cruz, CA); primary antibody for GAPDH was purchased from Cell Signaling Technology (Beverly, MA). Primers for PCR were purchased from Thermo Fisher Scientific (Waltham, MA).

### **2.2 Animals**

Adult male CD1 mice (age 6-8 weeks) were supplied by Charles River Laboratories; the mean body weight was about 33.7 g. Animal care and experiment protocols were approved by the Institutional Care and Use Committee (IACUC) of Virginia Commonwealth University (VCU).

### **2.3 Experimental Groups**

The CD1 mice were randomly divided between three groups: vehicle, positive control, and the experimental treatment. All three experimental groups were fed with standard chow prior to surgery. 1) After surgery, the vehicle group remained on standard chow for the duration of the experiment. The vehicle also received a normal saline injection at the time of reperfusion. 2) The positive control group also remained on standard chow for the duration of the experiment but received a supplemental intraperitoneal (IP) injection of 100 µg/kg sodium sulfide (Na<sub>2</sub>S) at the time of reperfusion as well as daily IP injections of 100 µg/kg Na<sub>2</sub>S. 3) The experimental treatment group received one injection of 100

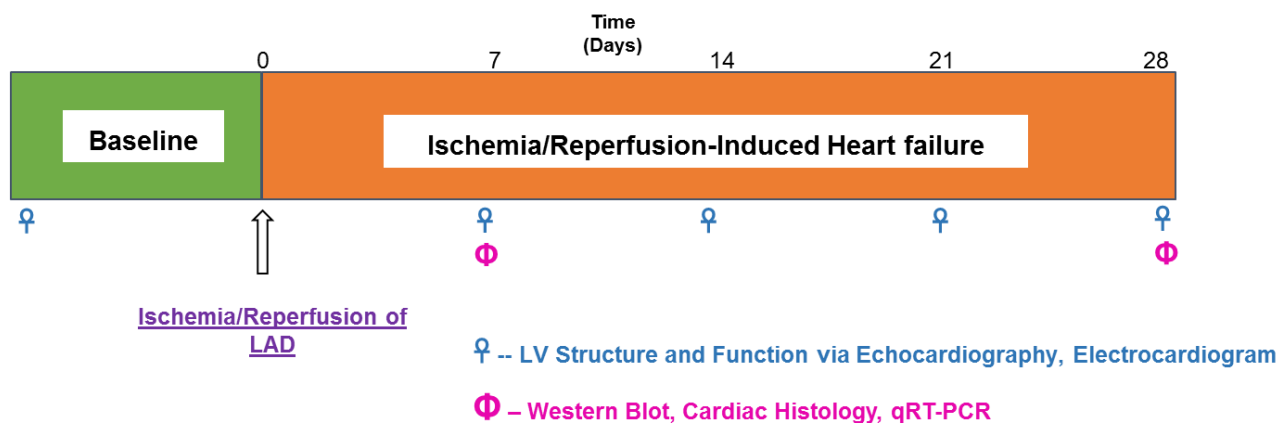


**Figure 4: Experimental Design.** CD1 Mice were subjected to ischemia/reperfusion surgery and were studied for a period of up to 28 days afterwards. Echocardiography and electrocardiography data was acquired weekly, while tissue for mRNA, protein, and histological analysis was collected only at 7 and 28 days post IR.



µg/kg Na<sub>2</sub>S at the time of reperfusion only. Following ischemia/reperfusion (I/R) surgery, the group was placed on the SG-1002 chow for the duration of the experiment.

## **2.4 Murine Ischemia/Reperfusion Model**

The CD1 mice were anesthetized with an intraperitoneal injection of pentobarbital. Additional doses of pentobarbital were given as needed to maintain anesthesia. The chest hair for each mouse was removed using Nair. The animals were then placed in a supine position on an operating platform with heating pads underneath. The mice were intubated by opening the animal's mouth, displacing the tongue from the airway, and inserting a 20 gauge catheter. The animals were placed on a ventilator at 133 respirations per minute, and the investigators monitored for adequate chest rise and fall at the appropriate rate to confirm placement in the trachea rather than the esophagus.

The ischemia/reperfusion (I/R) surgery was carried out under sterile conditions. A left thoracotomy was performed at the fourth intercostal space, and the heart was exposed after stripping the pericardium. A major branch of the left coronary artery was identified and occluded for 30 minutes by a 7-0 silk ligature that was placed around it and a small piece of polyethylene tubing (PE10) that was positioned on top of it. A successful occlusion was verified by visual inspection confirming the cyanosis and dyskinesia of the relevant segment of the left ventricle. After 30 minutes, the ligature and tube were removed, and blood flow was re-established. Prior to chest closing, air was expelled from the chest, and a sterile cotton tip was used to remove fluids from the thoracic cavity. The lungs were adequately inflated by blocking the ventilator exhaust for a few seconds to prevent the development of a pneumothorax. The chest was closed using a 5-0 silk suture, and the skin was closed using surgical clips. After completion of the surgery, the mice were closely observed during recovery until fully conscious and then extubated when they resumed spontaneous breathing. The animals received subcutaneous doses of an opioid analgesic (Buprenorphine SRLab 1.0 mg/kg) and intramuscular doses of an antibiotic (Gentamicin 0.7 mg/kg).

## **2.5 Echocardiography**

Transthoracic echocardiography was performed using the Vevo2100™ imaging system (VisualSonics Inc., Toronto, Canada) prior to surgery (baseline) and at the four weekly time points. Each mouse was placed in the supine position on a heating pad set to 37° C under anesthesia with isoflurane (2.0% to 3.0%) supplemented with 100% oxygen. Electrodes were applied to the limbs to obtain continuous ECG monitoring.

Parasternal Long Axis and Short Axis M-Mode images were obtained to assess LV function. The views were stored digitally in loops of 300 frames with depth, width and gain settings optimized. Short axis M-mode images were used to measure LV end-diastolic diameter (LVEDD) and LV end-systolic diameter (LVESD). LV fractional shortening (FS) was calculated as  $[(LVEDD - LVESD) / LVEDD] * 100$ . Long axis B-mode images were analyzed using Speckle Tracking Echocardiography (STE) software. This software identifies bright speckles in the ultrasound image and tracks them frame-by-frame to determine the strain, strain rate, velocity, and displacement of the various segments of the heart.

## **2.6 Measurement of Electrocardiographic Parameters**

Physiologic data from Vevo2100™ echocardiographic acquisition include outline of electrocardiographic (ECG) readings from limb leads. PR interval, QRS duration and QT interval calculations were done using LabChart Pro analysis of the ECG readings.

## **2.7 Western Blotting**

Protein was extracted from the frozen left ventricular tissue using 1x RIPA buffer (Cell Signaling Technology). Seventy-five (75 µg) protein from each sample was separated using 4-20% sodium-dodecyl sulfate polyacrylamide gel electrophoresis (SDS-PAGE) and then transferred onto a 0.2 µm pore-sized nitrocellulose membrane. The membrane was then incubated overnight at 4° C with primary antibody purchased from Santa Cruz Biotechnology (1:1000 dilution with 5% BSA). The membrane was then

washed and incubated with horseradish peroxidase (HRP) conjugated secondary antibody obtained from Sigma Aldrich (1:5000 dilution in 5% milk solution). A wet transfer method in 20% methanol/tris-glycine solution was used and the blots were developed using the LumiGlo chemiluminescent system (Cell Signaling Technology). Labeling of the individual proteins were done so after cutting the blot into separate sections based on their expected molecular weight.

## **2.8 Quantitative Real-Time PCR**

Total RNA was isolated from frozen hearts using miRNeasy mini kit according to manufacturer's protocol (QIAGEN Sciences, MD, USA). Concentration and purity of the isolated RNA was checked using Nanodrop ND-1000 spectrophotometer (Agilent technologies, CA, USA). 100 ng of RNA was converted to cDNA using the High Capacity cDNA Reverse Transcription kit (Life Technologies, Grand Island, NY, USA). Quantitative real-time PCR was performed using SYBR Green PCR master mix (Life Technologies) with a Roche 480 Thermocycler (Roche, Indianapolis, IN, USA). Gene expression was carried for the mRNAs for VEGF and Angiopoietin with Polr2a chosen as the housekeeping gene for comparison. In addition, Taqman based qRT-PCR was performed in order to investigate the change in microRNA-126 with U6 chosen as the housekeeping gene for comparison.

## **2.9 Histology**

For histological analysis, hearts were collected at 7 and 28 days post MI, fixed in 10% formalin, and embedded in paraffin. Serial 5- $\mu$ m heart sections were put onto microscope slides. After staining, coverslips were mounted.

### Capillary Density

Capillary density was measured using immunohistochemistry with a primary rabbit anti-caveolin and secondary anti-rabbit HRP-conjugate. Five fields of multiple sections from each cardiac tissue sample were randomly examined using a light microscope. The samples were blinded prior to photo

acquisition and analysis. The number of capillaries and cardiomyocytes in the non-infarct and peri-infarct regions were counted. A ratio of capillaries to cardiomyocytes was obtained for each picture, and the ratios were compared.

## **2.10 Data Analysis and Statistics**

All data are presented as mean  $\pm$  standard error of the mean (SEM). Data was tested for normality prior to statistical analysis. The differences between groups were analyzed using one-way analysis for comparison among three or more means. For the ANOVA, if statistical significance was found, the Tukey (1-way ANOVA) test was used for posthoc analysis.  $P < 0.05$  was considered to be statistically significant. All statistical analyses were performed using GraphPad Prism statistical software, Version 7.03 (La Jolla, California, USA).

## **Results**

### **3.1 Effect of H<sub>2</sub>S on LV Function**

To test the effect of H<sub>2</sub>S on LV function, echocardiography was performed prior to surgery and weekly following IR for up to 4 weeks. Left ventricular function as measured by LV ejection fraction (LVEF) from short axis M-mode tracings was significantly improved in both the Na<sub>2</sub>S treated group ( $52 \pm 3\%$ ,  $p=0.004$ ,  $n=10$ ) and the SG1002 ( $52 \pm 3\%$ ,  $p=0.005$ ,  $n=8$ ) treated group compared to vehicle ( $35 \pm 4\%$ ,  $n=10$ ) at 28 days post IR as displayed in Figure 5. Representative 28 day M-mode images of the various experimental groups are shown below the graph.

### **3.2 Effect of H<sub>2</sub>S on QRS interval**

Analysis of ECG tracings showed that H<sub>2</sub>S significantly preserved QRS interval in the Na<sub>2</sub>S group ( $10.53 \pm 0.44$  ms,  $p=0.0099$ ,  $n=10$ ) compared to the vehicle group ( $13.37 \pm 2.08$  ms,  $n=10$ ). There was also a trend of decreased QRS interval for the SG1002 group compared to the vehicle group. The results are displayed in Figure 6.

### **3.3 Effect of H<sub>2</sub>S on capillary density at 7 days and 28 days**

Capillary density measurements were taken using a microscope at 40X magnification. The infarct region at 7 days post IR showed a significant increase in capillaries and small vessels per high power field for SG1002 ( $30.04 \pm 0.66$ ,  $p=0.037$ ,  $n=3$ ) and Na<sub>2</sub>S ( $32.32 \pm 0.71$ ,  $p=0.009$ ,  $n=3$ ) treated mice compared to Vehicle ( $23.86 \pm 2.07$ ,  $n=5$ ). The infarct region at 7 days post IR results are displayed in Figure 7. SG1002 ( $41.1 \pm 3.5$ ,  $p=0.001$ ,  $n=3$ ) and Na<sub>2</sub>S ( $32.25 \pm 2.2$ ,  $p=0.005$ ,  $n=4$ ) treated mice displayed a significant increase in infarct-zone capillary density at 28 days compared to Vehicle ( $17.95 \pm 1.9$ ,  $n=4$ ). The infarct region at 28 days post IR results are displayed in Figure 8.

Measurements for the peri-infarct and non-infarct zones were taken as a function of capillaries normalized to the number of cardiomyocytes present in the field. Therefore, the data are presented as a ratio. Although there was no significance, there was an upward trend for the ratio of capillaries to

cardiomyocytes for both the Na<sub>2</sub>S and SG1002 groups compared to Vehicle in the peri-infarct zone at 28 days. Similarly, there was an upward trend for the Na<sub>2</sub>S and SG1002 compared to vehicle in the non-infarcted zone at 28 days. Peri-infarct 28 day results are displayed in Figure 9. Non-infarct 28 day results are displayed in Figure 10.

### **3.4 Effect of H<sub>2</sub>S on VEGF-A mRNA levels 28 days post IR**

mRNA for the hearts in each group was analyzed for VEGF levels. The SG1002 group showed a slight upward trend compared to Vehicle at 28 days post IR. The results are displayed in Figure 11.

### **3.5 Effect of H<sub>2</sub>S on Angiopoietin-1 mRNA levels at 28 days post IR**

Angiopoietin-1 signaling is another pro-angiogenic pathway that works concurrently with VEGF to promote proliferation and migration of endothelial progenitor cells. At 28 days, there is a slight upward trend for SG1002 compared to Vehicle. The results are shown in Figure 12.

### **3.6 Effect of H<sub>2</sub>S on microRNA-126 levels at 28 days post IR**

microRNA-126 (miR-126) was significantly upregulated in the SG1002 treatment group ( $1.962 \pm 0.045$ ,  $p=0.046$ ,  $n=3$ ) as compared to the vehicle group ( $1 \pm 0.08$ ,  $n=3$ ). The Na<sub>2</sub>S group also showed a non-significant upward trend compared to the control. The results are displayed in Figure 13.

### **3.7 Effect of H<sub>2</sub>S on VEGF-A protein levels at 7 and 28 days post IR**

VEGF-A levels at 7 days and 28 days post IR were analyzed by Western Blot to gauge the strength of the angiogenic signaling in the cardiomyocytes. At 7 days post IR, VEGF-A levels displayed an upward trend toward the H<sub>2</sub>S treated samples. The VEGF at 7 day post IR results are shown in Figure 14.

At 28 days post IR, SG1002 ( $2.37 \pm 0.32$ ,  $n=3$ ) showed a significant increase in VEGF-A when compared to both Sham ( $1.00 \pm 0.02$ ,  $p=0.007$ ,  $n=3$ ) and Vehicle ( $1.23 \pm 0.18$ ,  $p=0.02$ ,  $n=3$ ). The VEGF at 28 days post IR results are shown in Figure 15.

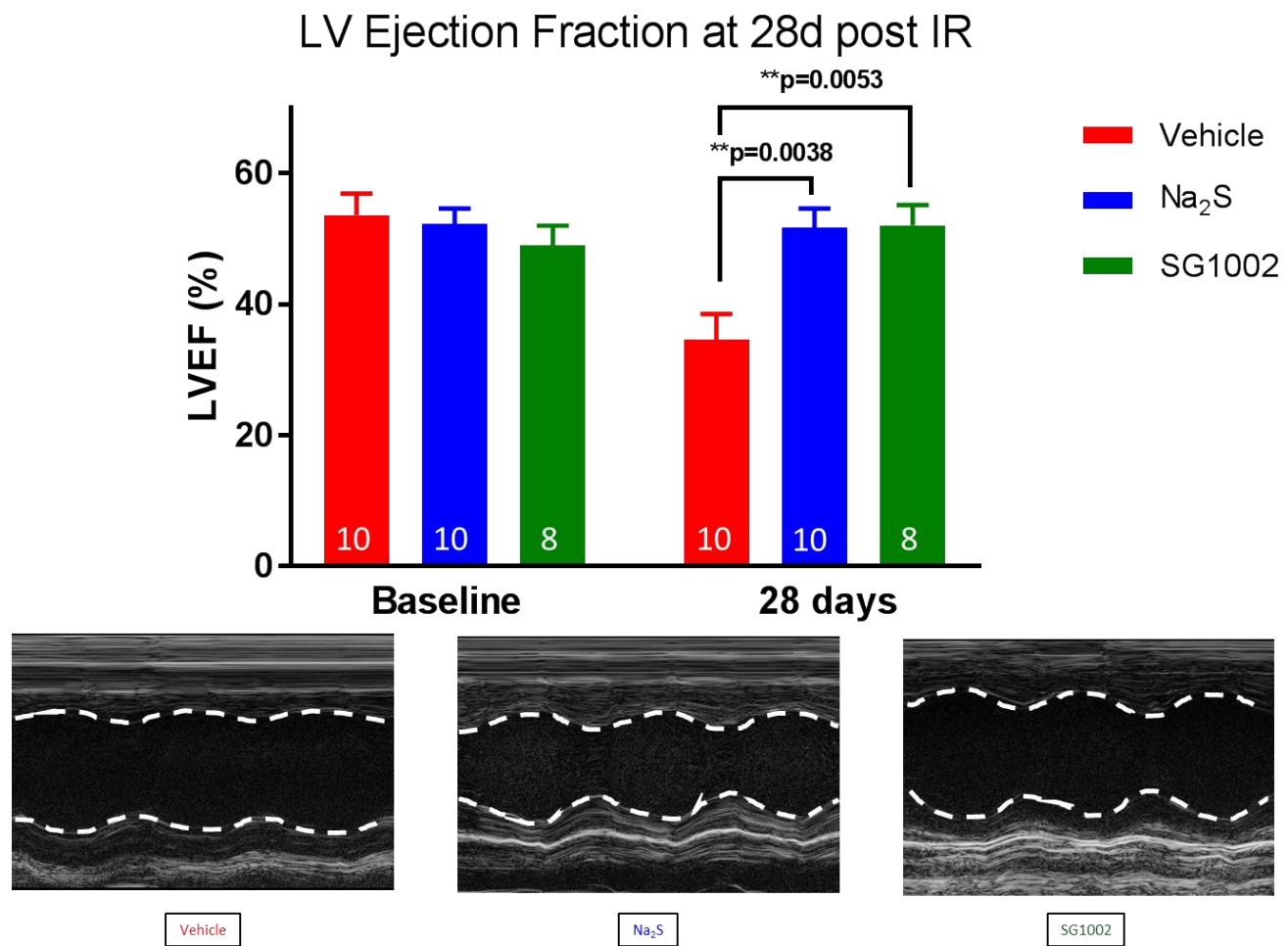


**Figure 5: H<sub>2</sub>S preserves ejection fraction at 28 days post IR.** Left Ventricular Ejection Fraction comparison and representative M-mode images of Vehicle and H<sub>2</sub>S treatment groups. LVEF was calculated from short-axis M-mode images using VevoSonic 2100.

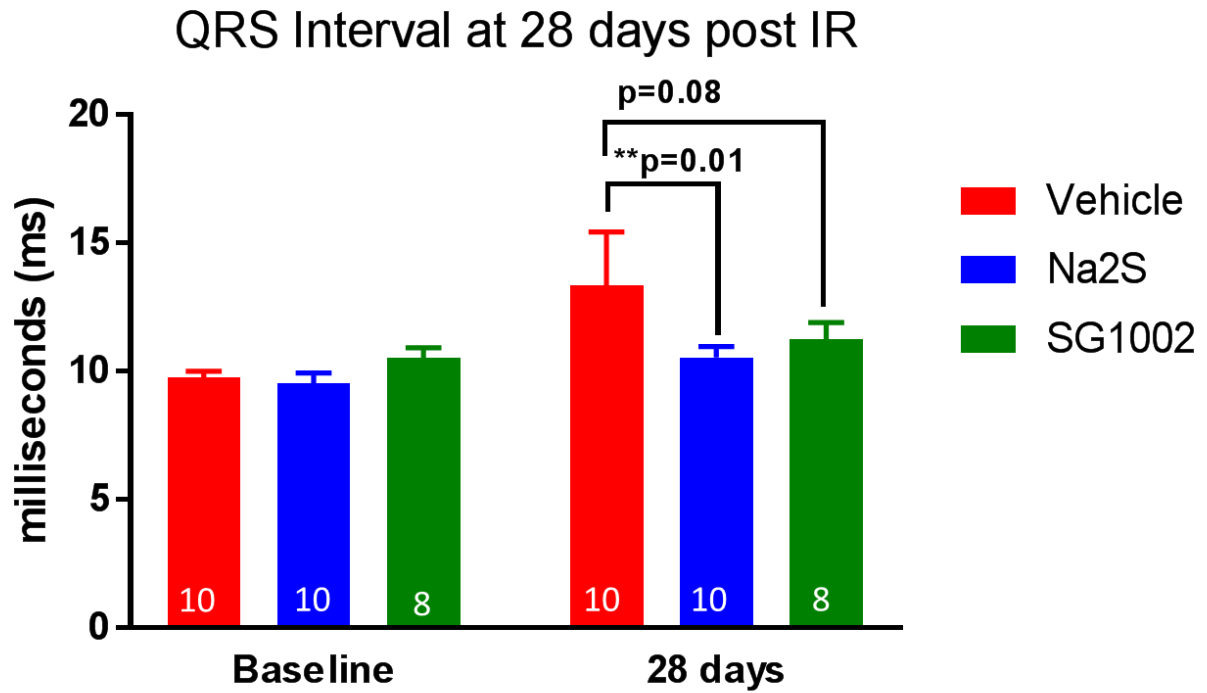
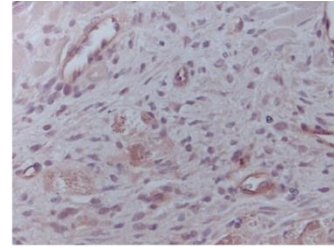
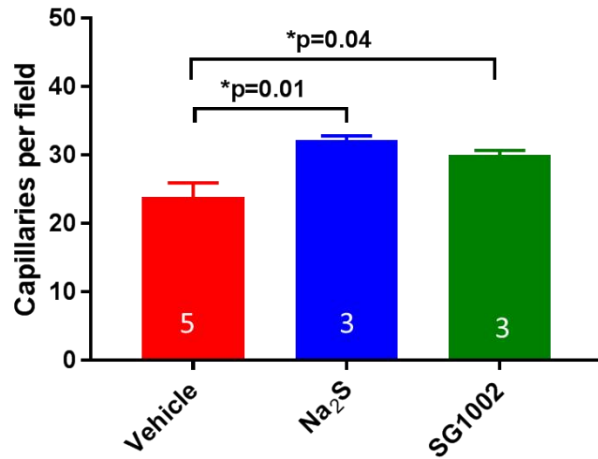


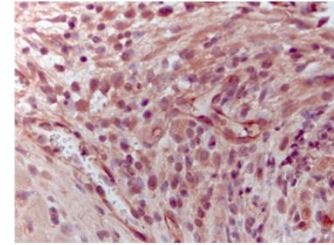
**Figure 6: H<sub>2</sub>S treatment attenuates QRS complex widening at 28 days post IR.** ECG analysis of the QRS intervals of H<sub>2</sub>S treatment groups, Na<sub>2</sub>S and SG1002, in comparison with Vehicle.



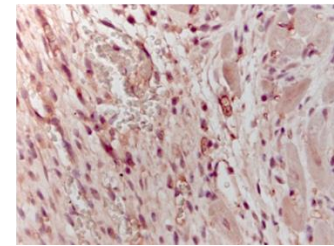
### Infarct Region Capillary Density at 7 days post IR



Vehicle



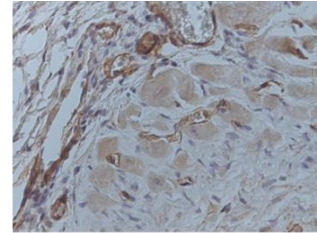
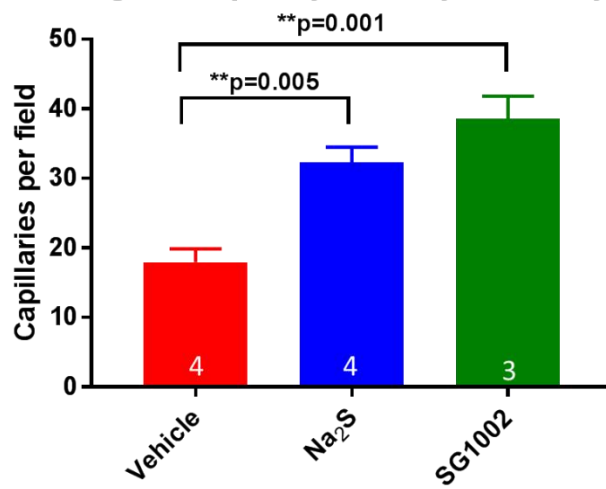
Na<sub>2</sub>S



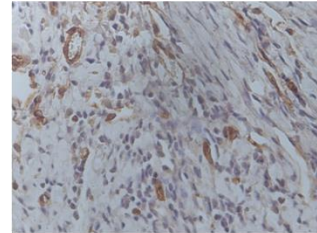
SG1002

**Figure 7: H<sub>2</sub>S therapy significantly increases capillary density at 7 days post IR.** Infarct region analysis of H<sub>2</sub>S treated mice and Vehicle. Representative images of caveolin-1 stained heart tissues from each group to reflect capillary density are shown to the right of the graph.

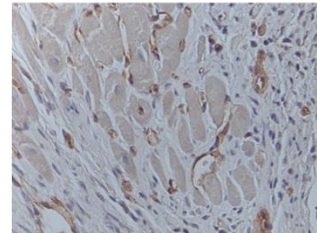
### Infarct Region Capillary Density at 28 days post IR



Vehicle



Na<sub>2</sub>S



SG1002

**Figure 8: H<sub>2</sub>S therapy significantly increases capillary density at 28 days post IR.** A) Infarct region analysis of H<sub>2</sub>S treated mice and Vehicle. Representative images of caveolin-1 stained heart tissues from each group to reflect capillary density are shown to the right of the graph.

## Peri-infarct Capillary Density at 28 days post IR

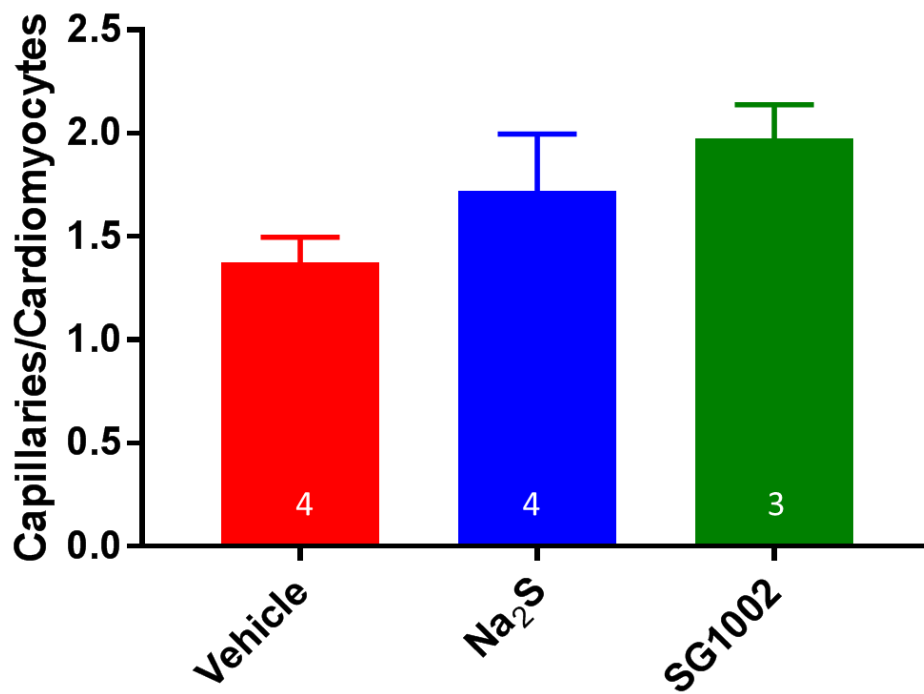


**Figure 9: H<sub>2</sub>S groups show an upward trend in peri-infarct region capillary density at 28 days post IR.** Peri-infarct region analysis of H<sub>2</sub>S treated mice compared to Vehicle. Data is presented as a ratio of capillaries in the microscopic area divided by the number of cardiomyocytes present.

## Non-infarct Capillary Density at 28 days post IR

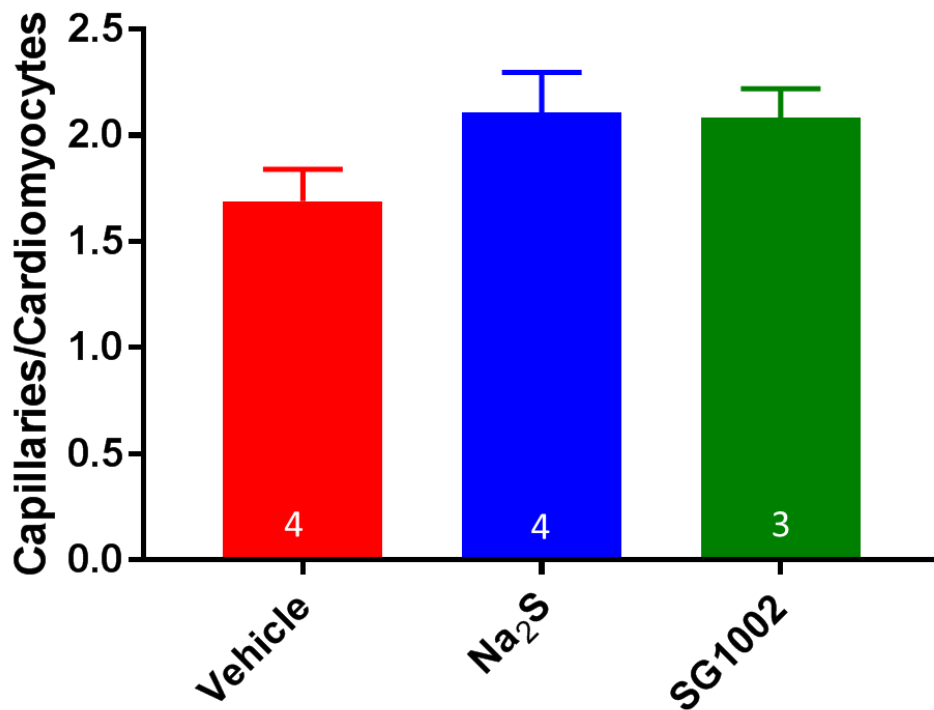


**Figure 10: H<sub>2</sub>S groups show an upward trend in non-infarct region capillary density at 28 days post IR.** Non-infarct region analysis of H<sub>2</sub>S treated mice compared to Vehicle. Data is presented as a ratio of capillaries in the microscopic area divided by the number of cardiomyocytes present.

## VEGF-A mRNA levels at 28 days post IR

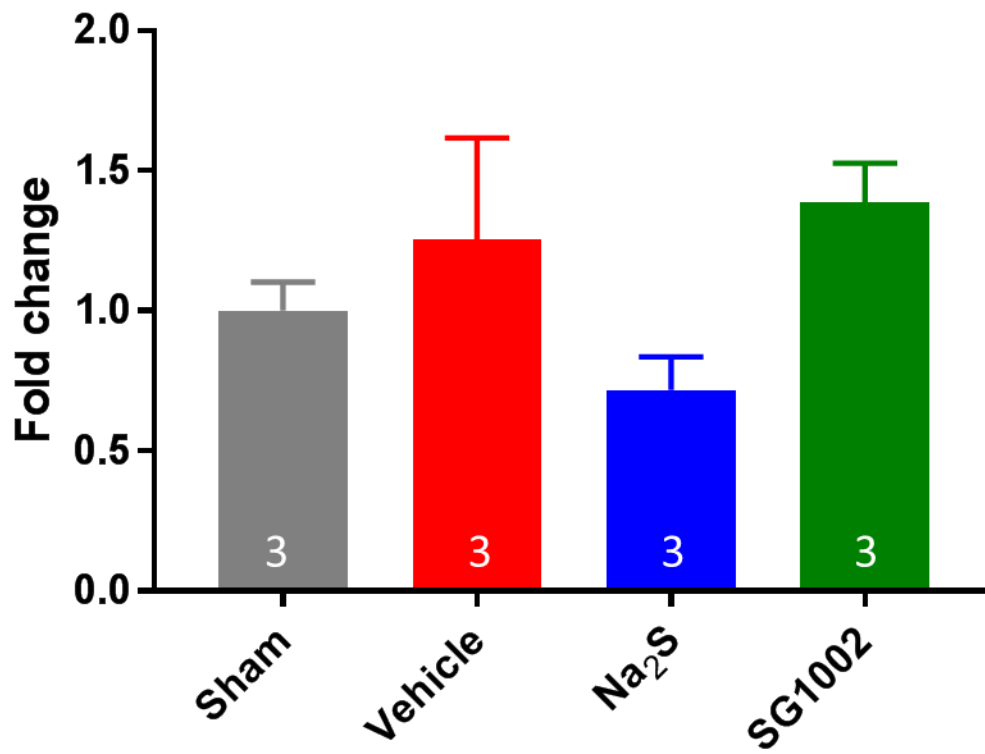


**Figure 11: SG1002 shows an upward trend in VEGF-A mRNA levels at 28 days post IR.** Comparison of the fold change values for VEGF-A mRNA between the different experimental groups.

## Angiotensin-1 mRNA levels at 28 days post IR

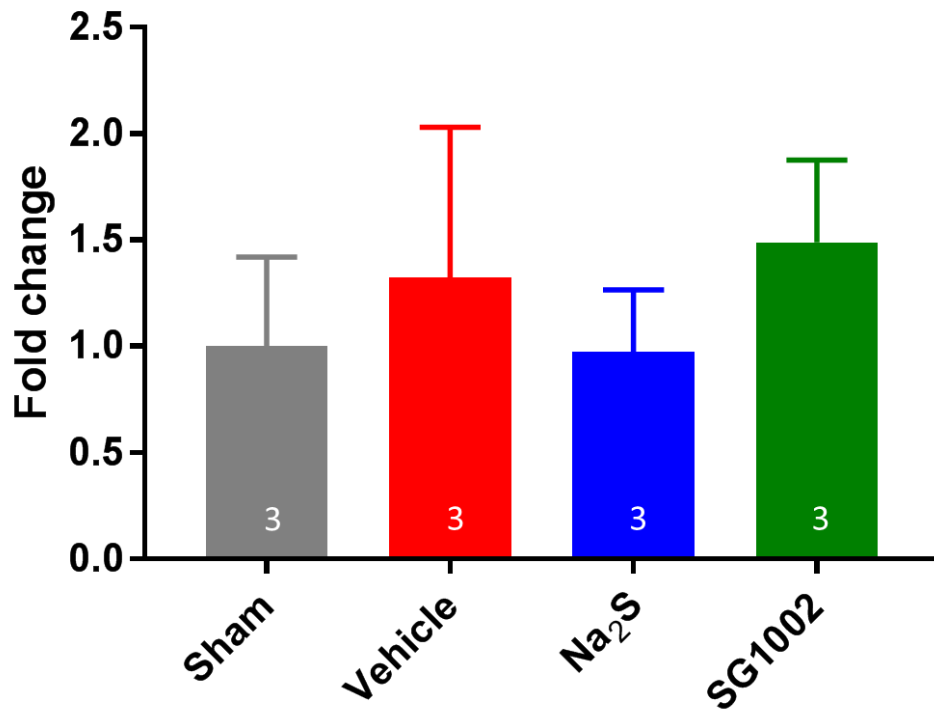


**Figure 12: SG1002 shows upward trend in Angiotensin-1 mRNA levels at 28 days post IR.** Comparison of the fold change values for Angiotensin-1 mRNA between the different experimental groups.

## miR-126 levels at 28 days post IR

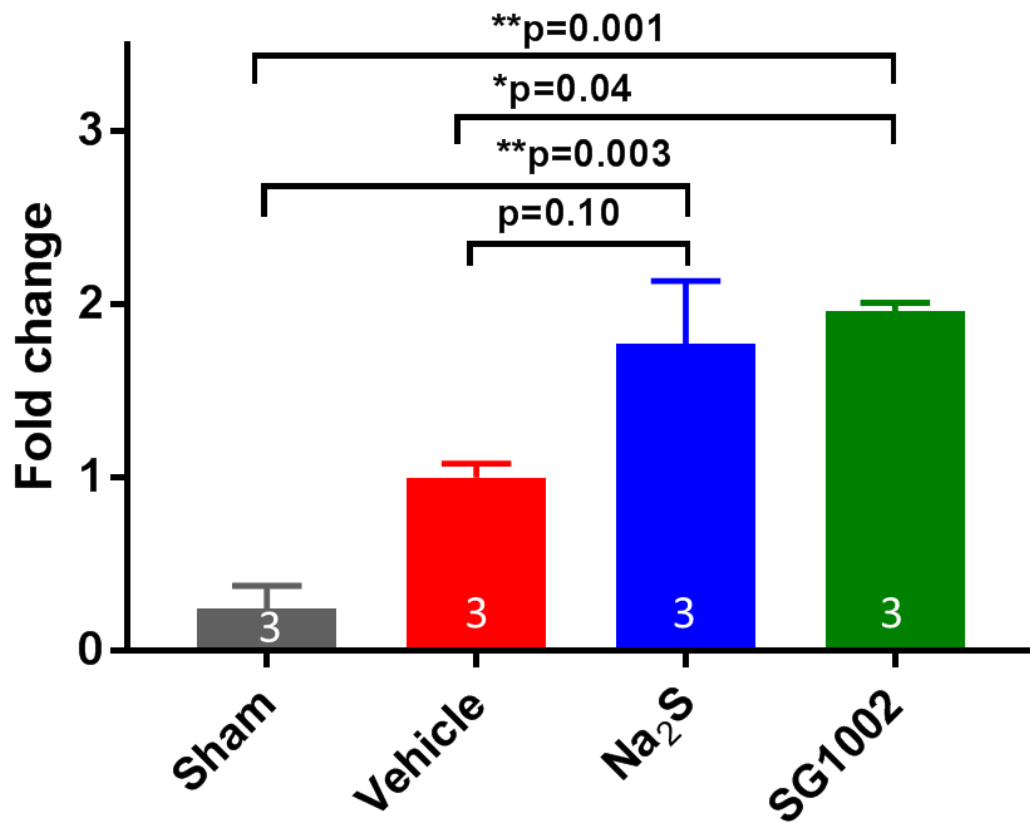


**Figure 13: SG1002 shows significant difference in microRNA-126 levels at 28 days post IR.** Comparison of the fold change values for microRNA-126 between the different experimental groups. n=3 for all groups.

## VEGF-A levels at 7 days post IR

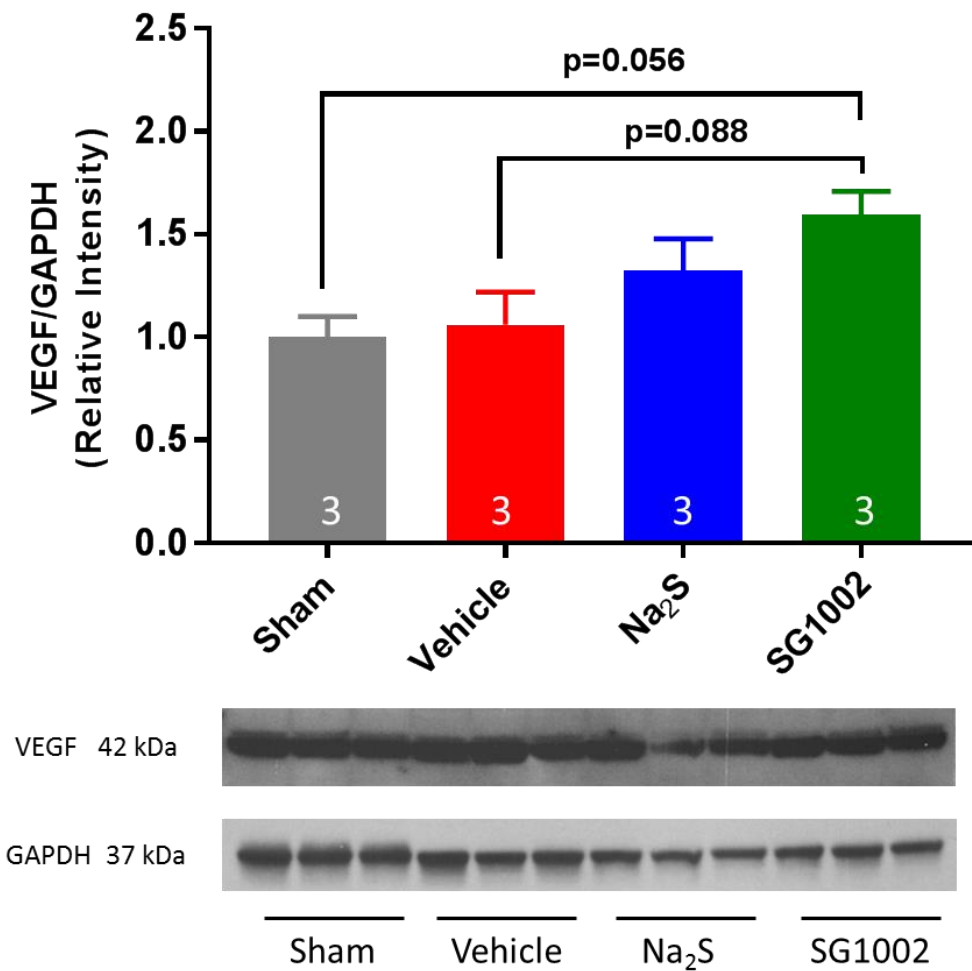


**Figure 14: H<sub>2</sub>S therapy increases VEGF-A protein expression at 7 days post IR.**

Densitometric analysis of the immunoblots for the ratio of VEGF/GAPDH, n=3 for all groups. Representative immunoblots for VEGF and GAPDH expression in the left ventricular tissue samples at 7 days after IR are shown below the graph.



## VEGF-A levels at 28 days post IR

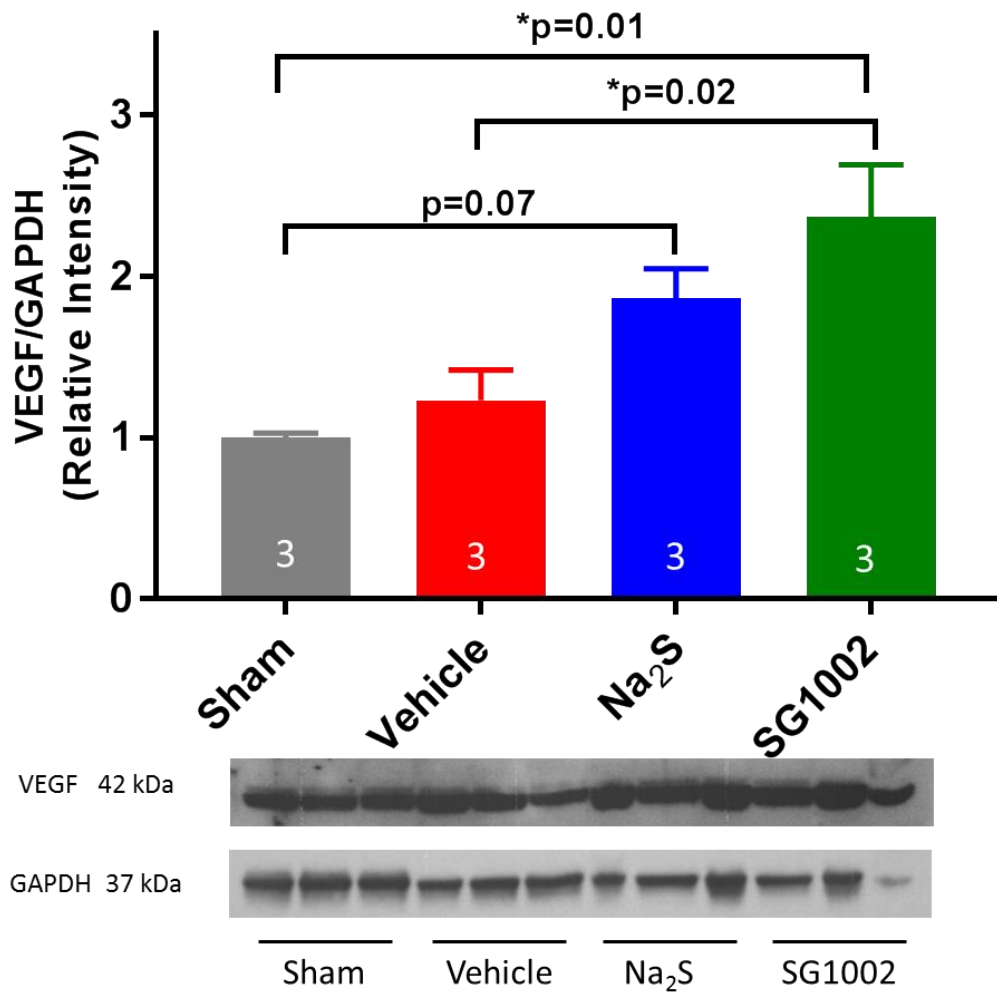


**Figure 15: H<sub>2</sub>S therapy increases VEGF-A protein expression at 28 days post IR.**

Densitometric analysis of the immunoblots for the ratio of VEGF/GAPDH; n=3 for all groups. Representative immunoblots for VEGF and GAPDH expression in the left ventricular tissue samples at 28 days after IR are shown below the graph.

## Discussion

The heart, and in particular the left ventricle, undergoes morphological changes in response to a myocardial injury. These changes, which result in remodeling of the chamber, begin as adaptive but progress to maladaptive in response to sustained stimuli. Following cardiac injury, the LV undergoes cell death, inflammation, oxidative stress, and fibrosis. These reactive processes stimulate each other and advance from acute cellular reactions to chronic anatomical and functional changes.<sup>61</sup> In the present study, we investigated the cardioprotective effects of hydrogen sulfide on the murine heart following ischemia/reperfusion injury. H<sub>2</sub>S has been associated with the regulation of cardiovascular homeostasis and the promotion of cellular signals that modulate metabolism, cardiac function, and cell survival.<sup>62</sup> Clinically, H<sub>2</sub>S plasma levels have been shown to be decreased in CAD patients compared to angiographically normal control subjects.<sup>31</sup> Therefore, multiple studies have explored the effects of exogenous H<sub>2</sub>S donors and their mechanisms of cardioprotection in the infarcted heart.<sup>6</sup>

Recent studies indicate that the heart progresses rapidly from compensated to decompensated failure when vascular growth cannot keep pace with the pathological hypertrophy of the myocyte.<sup>63</sup> This study specifically focused on the mechanisms of cardioprotection of two donors, Na<sub>2</sub>S and SG1002, through the induction of angiogenesis. Because H<sub>2</sub>S is a physiological gas that freely diffuses into multiple intracellular compartments, it is likely that H<sub>2</sub>S targets multiple pathological cascades simultaneously. In the cardiomyocyte, H<sub>2</sub>S can stimulate angiogenesis through the PI3K/Akt pathway, activation of K<sub>ATP</sub> channels, as well as activation of HIF-1 $\alpha$  to upregulate VEGF production.<sup>46</sup>

VEGF, in particular, plays an essential role in regulating multiple angiogenic cellular responses including survival, migration, and differentiation of endothelial cells. VEGF has been shown to be significantly increased in ischemic myocardium and immediately upregulated after coronary occlusion in the heart.<sup>64</sup> In cultured rat myocardial cells, mRNA levels of VEGF were significantly raised as early as 2-4 hours after exposure of cultures to hypoxia.<sup>65</sup> Moreover, in human tissue, steady-state levels of VEGF

mRNA were present in the initial periods of ischemia (<48 hours after onset) and in the intermediate periods of infarction (24 to 120 hours after onset).<sup>22</sup> In a rat model of left anterior descending (LAD) coronary ligation, VEGF mRNA levels remained elevated as late as 6 weeks following surgery.<sup>66</sup> In addition to the body's normal induction of VEGF mRNA levels, studies have demonstrated hydrogen sulfide's ability to further promote VEGF levels under hypoxic conditions.<sup>67</sup> In conjunction with these prior experiments, SG1002 therapy in the current study led to an upward trend in the mRNA for VEGF at 28 days in comparison to the vehicle group.

This increase in VEGF mRNA for SG1002 was also corroborated by increased protein expression of VEGF at 7 and 28 days following IR. There an upward trend in VEGF after 7 days when comparing both H<sub>2</sub>S donors to the Sham and Vehicle groups. On the other hand, there was a significant increase in VEGF in the SG1002 group at 28 days when compared to Sham and Vehicle, along with a non-significant upward trend when comparing the Na<sub>2</sub>S group to the sham. This is similar to data from other studies which investigated the effects of a different H<sub>2</sub>S donor, DATS, on VEGF levels after TAC.<sup>50</sup> Another study also demonstrated that SG1002 treatment activated a VEGF-Akt-eNOS-NO-cGMP signaling pathway following TAC.<sup>51</sup> Nevertheless, future work will be necessary to fully characterize the mechanisms that arise from activation of VEGF with SG1002 following IR.

Angiopoietins are another class of important pro-angiogenic factors along with VEGF. Over-expression of Angiopoietin-1 (Ang-1) has been shown to produce highly branched and leakage resistant blood vessels in the skin of transgenic mice. It also stimulates the formation of pericytes and smooth muscle cells with endothelial cells and helps to stabilize newly formed blood vessels.<sup>68</sup> A previous study employing repetitive ischemia of the LAD in a canine model showed a significant increase of Ang-1 mRNA at 21 days.<sup>69</sup> In a study of Type II diabetes using a murine model, hydrogen sulfide treatment was able to improve wound healing by restoration of endothelial progenitor cell function through an activation of Ang-1.<sup>70</sup> In this study, the SG1002 treatment group showed an upward trend of Ang-1

mRNA levels in comparison to the vehicle group. This is very important because Ang-1 and VEGF work together in order to promote the formation of mature and stable vessels.<sup>71</sup>

Micro-RNAs are also capable of influencing the angiogenic process, and microRNA-126 in particular was investigated in this study. miR-126 is highly expressed in heart and lung tissue, and it enhances the pro-angiogenic actions of VEGF and fibroblast growth factor (FGF) by promoting blood vessel formation.<sup>72</sup> The pro-angiogenic effect of miR-126 is attributed to the repression of Sprouty-related protein-1 (Sprd-1), an intracellular inhibitor of VEGF and FGF. In zebrafish, knockdown of miR-126 caused severe defects in vascular development, such as collapsed blood vessels and cranial bleeding.<sup>72</sup> miR-126 has even been shown to be downregulated in myocardial cells subjected to ischemia/reperfusion injury.<sup>73</sup> Additionally, increased plasma levels of miR-126 are negatively correlated with mortality in patients with ischemic cardiomyopathy.<sup>74</sup> However, up until this point, miR-126 has not been analyzed in regards to hydrogen sulfide's role in cardioprotection. In the current study, miR-126 was significantly elevated at 28 days in the SG1002 treatment group when compared to Vehicle, while the Na<sub>2</sub>S group showed an upward trend for miR-126 in comparison to Vehicle. This finding may help provide an insight into another protective mechanism of hydrogen sulfide that works in conjunction with its other pro-angiogenic targets.

This increase in these pro-angiogenic factors was also supported with an increase in capillary density in the H<sub>2</sub>S treated hearts. There was a significant increase in the infarcted region at 7 days for both H<sub>2</sub>S donors compared to Vehicle, while there was only a significant increase in the infarcted region for SG1002 at 28 days. Meanwhile, in the peri-infarcted region, the various groups showed little difference at 7 days, while exhibiting a non-significant upward trend for both H<sub>2</sub>S donors compared to Vehicle at 28 days. The infarct region data was paralleled in the TAC followed by DATS treatment study in which they found a significant increase in capillary density between the DATS and vehicle groups using

von Willebrand factor (vWF) and CD31 as markers for endothelial cells and Ki67 as the proliferation marker.<sup>50</sup>

The molecular changes observed in the cardiac tissue also translated into functional improvements based on transthoracic echocardiography and attenuation of QRS interval prolongation in both the Na<sub>2</sub>S and SG1002 groups. The left ventricular ejection fraction was significantly improved in the H<sub>2</sub>S treated groups compared to Vehicle at 28 days. Similar results of ejection fraction restoration have been noted with Na<sub>2</sub>S in ischemia-induced heart failure and with SG1002 following TAC.<sup>51,75</sup> Additionally, in this study, H<sub>2</sub>S showed the ability to significantly preserve the QRS interval in Na<sub>2</sub>S treated hearts compared to Vehicle. SG1002 showed a downward trend for QRS interval compared to Vehicle, despite no statistical significance. This further supports the notion that H<sub>2</sub>S helps to restore overall function since left-sided intraventricular conduction delay is associated with more advanced myocardial disease, worse LV function, poorer prognosis, and increased risk of ventricular tachyarrhythmias.<sup>76</sup> It is possible that H<sub>2</sub>S is preserving the function of key ion channels or gap junctions within the heart in order to attenuate the increase in QRS interval.

For future experimentation, we hope to delve deeper into the role of microRNA-126 in cardioprotection of the heart following H<sub>2</sub>S treatment. Spred-1 expression levels can be investigated in order to further interrogate the pathway through which miR-126 works. Another avenue can be to look at additional anti-angiogenic factors, such as Angiostatin, to check for their downregulation with H<sub>2</sub>S therapy. Finally, we can further research the mechanism behind hydrogen sulfide's effect on the QRS interval through channelopathy studies.

In this paper, we have provided novel insights into the complex mechanisms by which H<sub>2</sub>S treatment – either through a fast-releasing sodium salt in Na<sub>2</sub>S or through a novel, orally active, slow-releasing donor in SG1002 – can confer cardioprotective benefits in mitigating the progression to decompensated heart failure. We showed an upregulation of multiple pro-angiogenic factors such as

VEGF and Angiopoietin on the mRNA and protein levels following H<sub>2</sub>S treatment, and we also provided key insight into microRNA-126's involvement in the cardioprotective mechanism of hydrogen sulfide.

## References

1. Ziaeian B, Fonarow GC. Epidemiology and aetiology of heart failure. *Nat Rev Cardiol*. 2016;13(6):368-378. doi:10.1038/nrcardio.2016.25.
2. Benjamin EJ, Blaha MJ, Chiuve SE, et al. Heart Disease and Stroke Statistics-2017 Update: A Report From the American Heart Association. *Circulation*. 2017;135(10):e146-e603. doi:10.1161/CIR.0000000000000485.
3. Roger VL. Epidemiology of heart failure. *Circ Res*. 2013;113(6):646-659. doi:10.1161/CIRCRESAHA.113.300268.
4. Hausenloy DJ, Yellon DM. Myocardial ischemia-reperfusion injury: a neglected therapeutic target. *J Clin Invest*. 2013;123(1):92-100. doi:10.1172/JCI62874.
5. Ostadal B, Ostadalova I, Dhalla NS. Development of Cardiac Sensitivity to Oxygen Deficiency: Comparative and Ontogenetic Aspects. *Physiol Rev*. 1999;79(3):635-659. doi:10.1152/physrev.1999.79.3.635.
6. Salloum FN. Hydrogen sulfide and cardioprotection — Mechanistic insights and clinical translatability. *Pharmacol Ther*. 2015;152:11-17. doi:10.1016/j.pharmthera.2015.04.004.
7. Braunwald E. Heart Failure. *JACC Hear Fail*. 2013;1(1):1-20. doi:10.1016/j.jchf.2012.10.002.
8. Hochman JS, Healy Bulkley B. Expansion of Acute Myocardial Infarction: An Experimental Study. *Circ Res*. 1981;49(1):80-88.
9. Konstam MA, Kramer DG, Patel AR, Maron MS, Udelson JE. Left Ventricular Remodeling in Heart Failure. *JACC Cardiovasc Imaging*. 2011;4(1):98-108. doi:10.1016/j.jcmg.2010.10.008.
10. Cohn JN, Ferrari R, Sharpe N. Cardiac remodeling—concepts and clinical implications: a consensus paper from an international forum on cardiac remodeling. *J Am Coll Cardiol*. 2000;35(3):569-582. doi:10.1016/S0735-1097(99)00630-0.
11. Weisman HF, Bush DE, Mannisi JA, Bulkley BH. Global cardiac remodeling after acute myocardial infarction: A study in the rat model. *J Am Coll Cardiol*. 1985;5(6):1355-1362. doi:10.1016/S0735-1097(85)80348-X.
12. McKay RG, Pfeffer MA, Pasternak RC, et al. Left ventricular remodeling after myocardial infarction: a corollary to infarct expansion. *Circulation*. 1986;74(4):693-702. doi:10.1161/01.CIR.74.4.693.
13. Lilly LS. *Pathophysiology of Heart Disease*. 5th ed. Philadelphia: Wolters Kluwer; 2011.
14. Ware JA, Simons M. Angiogenesis in ischemic heart disease. *Nat Med*. 1997;3(2):158-164. doi:10.1038/nm0297-158.
15. Schaper W, Frenzel H, Hort W. Experimental coronary artery occlusion. *Basic Res Cardiol*.

- 1979;74(1):46-53. doi:10.1007/BF01907684.
16. Werb Z. ECM and Cell Surface Proteolysis: Regulating Cellular Ecology. *Cell*. 1997;91(4):439-442. doi:10.1016/S0092-8674(00)80429-8.
  17. Stetler-Stevenson WG. Matrix metalloproteinases in angiogenesis: a moving target for therapeutic intervention. *J Clin Invest*. 1999;103(9):1237-1241. doi:10.1172/JCI6870.
  18. Fisher C, Gilbertson-Beadling S, Powers EA, Petzold G, Poorman R, Mitchell MA. Interstitial Collagenase Is Required for Angiogenesis in Vitro. *Dev Biol*. 1994;162(2):499-510. doi:10.1006/dbio.1994.1104.
  19. Helm C-LE, Fleury ME, Zisch AH, Boschetti F, Swartz MA. Synergy between interstitial flow and VEGF directs capillary morphogenesis in vitro through a gradient amplification mechanism. *Proc Natl Acad Sci U S A*. 2005;102(44):15779-15784. doi:10.1073/pnas.0503681102.
  20. Soldi R, Mitola S, Strasly M, Defilippi P, Tarone G, Bussolino F. Role of  $\alpha v \beta 3$  integrin in the activation of vascular endothelial growth factor receptor-2. *EMBO J*. 1999;18(4):882-892.
  21. Tabibiazar R, Rockson S. Angiogenesis and the ischaemic heart. *Eur Heart J*. 2001;22(11):903-918. doi:10.1053/euhj.2000.2372.
  22. Lee SH, Wolf PL, Escudero R, Deutsch R, Jamieson SW, Thistlethwaite PA. Early Expression of Angiogenesis Factors in Acute Myocardial Ischemia and Infarction. *N Engl J Med*. 2000;342(9):626-633. doi:10.1056/NEJM200003023420904.
  23. JÜRGENSEN JS, ROSENBERGER C, WIESENER MS, et al. Persistent induction of HIF-1 $\alpha$  and -2 $\alpha$  in cardiomyocytes and stromal cells of ischemic myocardium. *FASEB J*. 2004;18(12):1415-1417. doi:10.1096/fj.04-1605fje.
  24. Krock BL, Skuli N, Simon MC. Hypoxia-induced angiogenesis: good and evil. *Genes Cancer*. 2011;2(12):1117-1133. doi:10.1177/1947601911423654.
  25. Cochain C, Channon KM, Silvestre J-S. Angiogenesis in the infarcted myocardium. *Antioxid Redox Signal*. 2013;18(9):1100-1113. doi:10.1089/ars.2012.4849.
  26. Li J, Hampton T, Morgan JP, Simons M. Stretch-induced VEGF Expression in the Heart. *J Clin Invest*. 1997;100(1):18-24.
  27. Lawrence M, McIntire L, Eskin S. Effect of flow on polymorphonuclear leukocyte/endothelial cell adhesion. *Blood*. 1987;70(5).
  28. Ando J, Tsuboi H, Korenaga R, et al. Shear stress inhibits adhesion of cultured mouse endothelial cells to lymphocytes by downregulating VCAM-1 expression.
  29. Wang R. Physiological Implications of Hydrogen Sulfide: A Whiff Exploration that Blossomed. *Physiol Rev*. 2012;92:791-896. doi:10.1152/physrev.00017.2011.
  30. Elrod JW, Calvert JW, Morrison J, et al. Hydrogen sulfide attenuates myocardial ischemia-



- reperfusion injury by preservation of mitochondrial function. *Proc Natl Acad Sci U S A*. 2007;104(39):15560-15565. doi:10.1073/pnas.0705891104.
31. Jiang H, Wu H, Li Z, Geng B, Tang C. [Changes of the new gaseous transmitter H<sub>2</sub>S in patients with coronary heart disease]. *Di Yi Jun Yi Da Xue Xue Bao*. 2005;25(8):951-954.
  32. Kovačić D, Glavnik N, Marinšek M, et al. Total Plasma Sulfide in Congestive Heart Failure. *J Card Fail*. 2012;18(7):541-548. doi:10.1016/J.CARDFAIL.2012.04.011.
  33. Sodha NR, Clements RT, Feng J, et al. The effects of therapeutic sulfide on myocardial apoptosis in response to ischemia-reperfusion injury. *Eur J Cardiothorac Surg*. 2008;33(5):906-913. doi:10.1016/j.ejcts.2008.01.047.
  34. Cicconi S, Ventura N, Pastore D, et al. Characterization of apoptosis signal transduction pathways in HL-5 cardiomyocytes exposed to ischemia/reperfusion oxidative stress model. *J Cell Physiol*. 2003;195(1):27-37. doi:10.1002/jcp.10219.
  35. Shi S, Li Q, Li H, et al. Anti-apoptotic action of hydrogen sulfide is associated with early JNK inhibition. *Cell Biol Int*. 2009;33(10):1095-1101. doi:10.1016/j.cellbi.2009.06.029.
  36. Guo R, Lin J, Xu W, et al. Hydrogen sulfide attenuates doxorubicin-induced cardiotoxicity by inhibition of the p38 MAPK pathway in H9c2 cells. *Int J Mol Med*. 2013;31(3):644-650. doi:10.3892/ijmm.2013.1246.
  37. Li H, Zhang C, Sun W, et al. Exogenous hydrogen sulfide restores cardioprotection of ischemic post-conditioning via inhibition of mPTP opening in the aging cardiomyocytes. *Cell Biosci*. 2015;5. doi:10.1186/s13578-015-0035-9.
  38. Toldo S, Das A, Mezzaroma E, et al. Induction of microRNA-21 with exogenous hydrogen sulfide attenuates myocardial ischemic and inflammatory injury in mice. *Circ Cardiovasc Genet*. 2014;7(3):311-320. doi:10.1161/CIRCGENETICS.113.000381.
  39. Rani V, Yadav UCS. *Free Radicals in Human Health and Disease*.
  40. Calvert JW, Jha S, Gundewar S, et al. Hydrogen sulfide mediates cardioprotection through Nrf2 signaling. *Circ Res*. 2009;105(4):365-374. doi:10.1161/CIRCRESAHA.109.199919.
  41. Peake BF, Nicholson CK, Lambert JP, et al. Hydrogen sulfide preconditions the *db/db* diabetic mouse heart against ischemia-reperfusion injury by activating Nrf2 signaling in an Erk-dependent manner. *Am J Physiol Circ Physiol*. 2013;304(9):H1215-H1224. doi:10.1152/ajpheart.00796.2012.
  42. Sun W-H, Liu F, Chen Y, Zhu Y-C. Hydrogen sulfide decreases the levels of ROS by inhibiting mitochondrial complex IV and increasing SOD activities in cardiomyocytes under ischemia/reperfusion. *Biochem Biophys Res Commun*. 2012;421(2):164-169. doi:10.1016/J.BBRC.2012.03.121.
  43. Frangogiannis NG. The inflammatory response in myocardial injury, repair, and remodelling. *Nat Rev Cardiol*. 2014;11(5):255-265. doi:10.1038/nrcardio.2014.28.

44. Franchi L, Eigenbrod T, Muñoz-Planillo R, Nuñez G. The inflammasome: a caspase-1-activation platform that regulates immune responses and disease pathogenesis. *Nat Immunol.* 2009;10(3):241-247. doi:10.1038/ni.1703.
45. Pan H, Chen D, Liu B, Xie X, Zhang J, Yang G. Effects of sodium hydrosulfide on intestinal mucosal injury in a rat model of cardiac arrest and cardiopulmonary resuscitation. *Life Sci.* 2013;93(1):24-29. doi:10.1016/J.LFS.2013.05.012.
46. CAI W, WANG M, MOORE P, JIN H, YAO T, ZHU Y. The novel proangiogenic effect of hydrogen sulfide is dependent on Akt phosphorylation. *Cardiovasc Res.* 2007;76(1):29-40. doi:10.1016/j.cardiores.2007.05.026.
47. Papapetropoulos A, Pyriochou A, Altaany Z, et al. Hydrogen sulfide is an endogenous stimulator of angiogenesis. *Proc Natl Acad Sci U S A.* 2009;106(51):21972-21977. doi:10.1073/pnas.0908047106.
48. Wang M-J, Cai W-J, Li N, Ding Y-J, Chen Y, Zhu Y-C. The Hydrogen Sulfide Donor NaHS Promotes Angiogenesis in a Rat Model of Hind Limb Ischemia. *Antioxid Redox Signal.* 2010;12(9):1065-1077. doi:10.1089/ars.2009.2945.
49. Givvimani S, Munjal C, Gargoum R, et al. Hydrogen sulfide mitigates transition from compensatory hypertrophy to heart failure. *J Appl Physiol.* 2011;110(4):1093-1100. doi:10.1152/jappphysiol.01064.2010.
50. Polhemus D, Kondo K, Bhushan S, et al. Hydrogen sulfide attenuates cardiac dysfunction after heart failure via induction of angiogenesis. *Circ Heart Fail.* 2013;6(5):1077-1086. doi:10.1161/CIRCHEARTFAILURE.113.000299.
51. Kondo K, Bhushan S, King AL, et al. H<sub>2</sub>S protects against pressure overload-induced heart failure via upregulation of endothelial nitric oxide synthase. *Circulation.* 2013;127(10):1116-1127. doi:10.1161/CIRCULATIONAHA.112.000855.
52. Ji Y, Pang Q, Xu G, Wang L, Wang J, Zeng Y. Exogenous hydrogen sulfide postconditioning protects isolated rat hearts against ischemia-reperfusion injury. *Eur J Pharmacol.* 2008;587(1-3):1-7. doi:10.1016/J.EJPHAR.2008.03.044.
53. DeLeon ER, Stoy GF, Olson KR. Passive loss of hydrogen sulfide in biological experiments. *Anal Biochem.* 2012;421(1):203-207. doi:10.1016/J.AB.2011.10.016.
54. Papapetropoulos A, Whiteman M, Cirino G. Pharmacological tools for hydrogen sulphide research: a brief, introductory guide for beginners. *Br J Pharmacol.* 2015;172(6):1633-1637. doi:10.1111/bph.12806.
55. Predmore BL, Kondo K, Bhushan S, et al. The polysulfide diallyl trisulfide protects the ischemic myocardium by preservation of endogenous hydrogen sulfide and increasing nitric oxide bioavailability. *Am J Physiol Circ Physiol.* 2012;302(11):H2410-H2418. doi:10.1152/ajpheart.00044.2012.
56. Zheng Y, Ji X, Ji K, Wang B, Pharmaceutica Sinica AB. Hydrogen sulfide prodrugs—a review. *Acta*

- Pharm Sin B*. 2015;5(5):367-377. doi:10.1016/j.apsb.2015.06.004.
57. Li L, Whiteman M, Guan YY, et al. Characterization of a novel, water-soluble hydrogen sulfide-releasing molecule (GYY4137): new insights into the biology of hydrogen sulfide. *Circulation*. 2008;117(18):2351-2360. doi:10.1161/CIRCULATIONAHA.107.753467.
  58. Donnarumma E, Trivedi RK, Lefer DJ, Donnarumma E, Trivedi RK, Lefer DJ. Protective Actions of H<sub>2</sub>S in Acute Myocardial Infarction and Heart Failure. In: *Comprehensive Physiology*. Hoboken, NJ, USA: John Wiley & Sons, Inc.; 2017:583-602. doi:10.1002/cphy.c160023.
  59. Wallace JL, Vaughan D, Dickey M, Macnaughton WK, De Nucci G. Hydrogen Sulfide-Releasing Therapeutics: Translation to the Clinic. doi:10.1089/ars.2017.7068.
  60. Polhemus DJ, Li Z, Pattillo CB, et al. A Novel Hydrogen Sulfide Prodrug, SG1002, Promotes Hydrogen Sulfide and Nitric Oxide Bioavailability in Heart Failure Patients. *Cardiovasc Ther*. 2015;33(4):216-226. doi:10.1111/1755-5922.12128.
  61. Polhemus D, Kondo K, Bhushan S, et al. Hydrogen sulfide attenuates cardiac dysfunction after heart failure via induction of angiogenesis. *Circ Heart Fail*. 2013;6(5):1077-1086. doi:10.1161/CIRCHEARTFAILURE.113.000299.
  62. Salloum FN, Chau VQ, Hoke NN, et al. Phosphodiesterase-5 inhibitor, tadalafil, protects against myocardial ischemia/reperfusion through protein-kinase g-dependent generation of hydrogen sulfide. *Circulation*. 2009;120(11 Suppl):S31-6. doi:10.1161/CIRCULATIONAHA.108.843979.
  63. Izumiya Y, Shiojima I, Sato K, Sawyer DB, Colucci WS, Walsh K. Vascular endothelial growth factor blockade promotes the transition from compensatory cardiac hypertrophy to failure in response to pressure overload. *Hypertens (Dallas, Tex 1979)*. 2006;47(5):887-893. doi:10.1161/01.HYP.0000215207.54689.31.
  64. Hashimoto E, Ogita T, Nakaoka T, Matsuoka R, Takao A, Kira Y. Rapid induction of vascular endothelial growth factor expression by transient ischemia in rat heart. *Am J Physiol - Hear Circ Physiol*. 1994;267(5):H1948-H1954.
  65. Banai S, Shweiki D, Pinson A, Chandra M, Lazarovici G, Keshet E. Upregulation of vascular endothelial growth factor expression induced by myocardial ischaemia: implications for coronary angiogenesis. *Cardiovasc Res*. 1994;28(8):1176-1179.
  66. Brown LF, Hibberd MG, Grossman JD, Morgan JP, Grossman JD, Si M. VEGF, flk-1, and fit-1 expression in a rat myocardial infarction model of angiogenesis.
  67. Liu X, Pan L, Zhuo Y, Gong Q, Rose P, Zhu Y. Hypoxia-Inducible Factor-1 $\alpha$  Is Involved in the Pro-angiogenic Effect of Hydrogen Sulfide under Hypoxic Stress. *Biol Pharm Bull*. 2010;33(9):1550-1554. doi:10.1248/bpb.33.1550.
  68. Suri C, McClain J, Thurston G, et al. Increased vascularization in mice overexpressing angiopoietin-1. *Science*. 1998;282(5388):468-471.
  69. Matsunaga T, Warltier DC, Tessmer J, Weihrauch D, Simons M, Chilian WM. Expression of VEGF

- and angiopoietins-1 and -2 during ischemia-induced coronary angiogenesis. *Am J Physiol Circ Physiol*. 2003;285(1):H352-H358. doi:10.1152/ajpheart.00621.2002.
70. Liu F, Chen D-D, Sun X, et al. Hydrogen sulfide improves wound healing via restoration of endothelial progenitor cell functions and activation of angiopoietin-1 in type 2 diabetes. *Diabetes*. 2014;63(5):1763-1778. doi:10.2337/db13-0483.
  71. Tao Z, Chen B, Tan X, et al. Coexpression of VEGF and angiopoietin-1 promotes angiogenesis and cardiomyocyte proliferation reduces apoptosis in porcine myocardial infarction (MI) heart. *Proc Natl Acad Sci U S A*. 2011;108(5):2064-2069. doi:10.1073/pnas.1018925108.
  72. Wang S, Aurora AB, Johnson BA, et al. The Endothelial-Specific MicroRNA miR-126 Governs Vascular Integrity and Angiogenesis. doi:10.1016/j.devcel.2008.07.002.
  73. Li B, Tao Y, Huang Q. Effect and mechanism of miR-126 in myocardial ischemia reperfusion. *funpecrp.com.br Genet Mol Res Mol Res*. 2015;14(144):18990-18998. doi:10.4238/2015.December.29.6.
  74. Qiang L, Hong L, Ningfu W, Huaihong C, Jing W. Expression of miR-126 and miR-508-5p in endothelial progenitor cells is associated with the prognosis of chronic heart failure patients. *Int J Cardiol*. 2013;168(3):2082-2088. doi:10.1016/j.ijcard.2013.01.160.
  75. Shimizu Y, Nicholson CK, Lambert JP, et al. Sodium Sulfide Attenuates Ischemic-Induced Heart Failure by Enhancing Proteasomal Function in an Nrf2-Dependent Manner. *Circ Heart Fail*. 2016;9(4):e002368. doi:10.1161/CIRCHEARTFAILURE.115.002368.
  76. Kashani A, Barold SS. Significance of QRS Complex Duration in Patients With Heart Failure. *J Am Coll Cardiol*. 2005;46(12):2183-2192. doi:10.1016/J.JACC.2005.01.071.